SUPEROXIDE DISMUTASE INHIBITOR SCREENING AND CHARACTERIZATION USING ^{19}F NMR

A thesis presented to the faculty of the Graduate School of
Western Carolina University in partial fulfillment of the
requirements for the degree of Master of Science in Chemistry.

By

Megan Elizabeth Arrington

Director: Dr. Jack Summers
Assistant Professor of Chemistry
Department of Chemistry & Physics

Committee Members: Dr. Jeff Schmitt
Dr. Scott Huffman, Chemistry
Dr. Lori Seischab, Biology

March 2010

ACKNOWLEDGEMENTS

I would like to thank my committee members and my director for their assistance. In particular, Dr. Jack Summers for giving me the opportunity to work on this project and for his guidance and patience in its completion; Dr. Jeff Schmitt, for his hard work and assistance in docking calculations; and Dr. Lori Seischab and Emily Jellen-McCullough for their continued support. I express thanks to the research group members who contributed to this project: Jonathan Markley, Michelle Yost, Jessica Parris, Ben Hickman, Amanda Nance and Corey Harrington.

Many people assisted in this project and I appreciate their hard work. Dr. Scott Huffman calculated pK_a values for galangin and assisted in UV-Vis Spectroscopy. Dr. Carmen Huffman assisted in Spartan '04 calculations. Dr. David Evanoff of Western Carolina University and Michael Samuel of Wake Forest University analyzed Mass Spectrometry samples. Brian Sneed and Dr. Brian Dinkelmeyer purified chalcones. Amy Freund of the Bruker BioSpin Corporation performed NMR high throughput screening. Thank you again for all you have provided to this project.

I also would like to thank Dr. Jeff Schmitt and Bent Creek Institute for the use of computational software and Dr. Lori Seischab for the assistance and use of UV-Vis spectrometer microplate reader. I appreciate the compounds provided by Dr. William Kwochka and Dr. Scott Huffman, and the Chemical Methodologies and Library Development Center at the University of Pittsburgh.

I would like to give special thanks to the North Carolina Biotechnology Center for the basic research grant, which supported this project. Finally, I am grateful to the faculty of the Department of Chemistry and Physics, Western Carolina University, and my family for their continued encouragement in my coursework and research.

TABLE OF CONTENTS

LIST OF TABLES

LIST OF FIGURES

LIST OF ABBREVIATIONS AND SYMBOLS

2ME	2-Methoxyestradiol
4HAP/di-OH	4-Hydroxyacetophenone
$A/A_0/\%SOD_{Ac}$	Activity/ Initial Activity/ Percent Activity
Abs	Absorbance
ACA	9-Anthracenecarboxylic acid
Arg	Arginine
C_1/C_2	Constants based on fluoride resonance sensitivity to relaxation by the enzyme, the delay, and F^- and tfa concentration
CPMG	Carr-Purcell-Meiboom-Gill
CuZnSOD	Copper-Zinc Superoxide Dismutase
DHCH	N-N-(1,2-Dihydroxycyclohex-1,2-ylene)-L-Arginine
DMSO	Dimethylsulfoxide
eHiTS	Electronic High Throughput Screening
FeSOD	Iron Superoxide Dismutase
HEPES	N-[2-Hydroxyethyl]piperazine-N'-[2-Ethanesulfonic acid]
HTS	High Throughput Screening
I/I_0	NMR Resonance Integral/ Initial Resonance Integral
IC_{50}	Half Maximal Inhibitory Concentration
Inh	Inhibitor (Monomer)
Inh_2	Inhibition Dimer
Inh_{Tot}	Total/Experimental Inhibitor Concentration
k	Rate Constant for R_2 NMR Relaxation Rate
K_1	Association Binding Constant
k_2	Rate Constant for Inhibition Step 2
k_{app}	Apparent Rate Constant
$K_d/K_{d,max}$	Dissociation Constant/ Experimental Dissociation Constant
K_{dim}	Dimerization Constant
k_{obs}	Observed Rate Constant
Kaemp	Kaempferol
Lys	Lysine
MnSOD	Manganese Superoxide Dismutase
Myr	Myricetin
NADH	Nicotinamide Adenine Dinucleotide
NBT	Nitroblue Tetrazolium
PIPES	Piperazine-N,N'-bis(2-Ethanesulfonic Acid)
PMS	Phenazine Methosulfate
R_2	NMR Transverse Relaxation Rate
$\%SOD_{InAc}$	Percent of Inactive SOD
SOD	Superoxide Dismutase
τ	Delay Time
t	Time
T_1	Spin Lattice Relaxation Rate Constant
T_2	Spin-Spin Relaxation Rate Constant
TEA	Triethylamine
tfa	Trifluoroacetate

THAP/tri-OH 2,4,6-Trihydroxyacetophenone
Thr..... Threonine
Tris ..... Tris(hydroxymethyl)aminomethane

ABSTRACT

SUPEROXIDE DISMUTASE INHIBITOR SCREENING AND CHARACTERIZATION USING ^{19}F NMR

Megan Elizabeth Arrington, M.S.

Western Carolina University (March 2010)

Director: Jack Summers, Ph.D.

Superoxide dismutase enzymes (SOD) catalyze the disproportionation of superoxide to form molecular oxygen and hydrogen peroxide in a cyclic mechanism. SODs prevent the formation of hydroxyl radicals, preventing apoptosis. Up-regulation of this enzyme implicates it in the survival of cancer cells and pathogenic bacteria, leading to a call for SOD inhibitors as potential drugs. ^{19}F NMR based assays were used to study inhibition of CuZnSOD by flavonol compounds. Flavonols are more effective inhibitors at high pH. We hypothesize that inhibition at high pH occurs through a two-step reaction, where the first step is an equilibrium reaction affected by the deprotonation of the inhibitor and the second step is slower and affected by the deprotonation of the enzyme. The pH dependence of the second inhibition step is consistent with enzyme deprotonation of active site Lys 122 at pH=10.1 and is not necessary for the first step. It was also observed that aggregation of flavonol inhibitors may be occurring and therefore flavonol binding is stronger than experimentally measured.

To understand the factors that affect binding of flavonols to CuZnSOD, AutoDock 4.0 calculations were carried out and compared to experimental binding constants at pH 8. Experimental binding data show that flavonol diketone tautomerization is not necessary for binding and that inhibitors bind more effectively above their pK_{a1} values.

Bis-deprotonated, enol and S-diketone tautomers were predicted to bind CuZnSOD preferentially in docking results. Computational results indicate that lysine and arginine residues contribute significantly to binding by hydrogen bonding with flavonol 3,7, and 4'-oxygens. Despite a strong overall correlation between docking scores for the deprotonated species and experimental results, apigenin was predicted to have a higher binding affinity than is experimentally observed. The underlying cause of this discrepancy is a matter of further investigation.

1. INTRODUCTION

1.A. Superoxide

Superoxide is a radical anion produced by metabolic pathways in the body through the reduction of molecular oxygen.[1] After it is produced, superoxide can react with other biological molecules by either univalent oxidation or reduction.[2] It may also form the hydroxyl radical through the Fenton reaction, where superoxide acts by reducing iron as shown in Equation 1A and 1B.[3]

$$O_2^{\cdot -} + Fe^{3+} \rightarrow O_2 + Fe^{2+} \quad (1A)$$

$$H_2O_2 + Fe^{2+} \rightarrow {}^{\cdot}OH + OH^- + Fe^{3+} \quad (1B)$$

The hydroxyl radical is a reactive oxygen species, which can modify nucleic acids and proteins through oxidation. The formation of reactive oxygen species by superoxide leads to oxidative stress.[1]

1.B. Superoxide Dismutase

Superoxide is a natural product of aerobic metabolism and is often produced in large quantities (10^7 radicals per day in rat mitochondria)[1] therefore; a reaction of superoxide must be present to protect the cell from damage.[4] The superoxide dismutation reaction was first proposed by McCord and Fridovich[4] and is shown in Equation 2.

$$O_2^{\cdot -} + O_2^{\cdot -} + 2H^+ \rightarrow O_2 + H_2O_2 \quad (2)$$

In the dismutation reaction, one superoxide molecule is oxidized and the other is reduced resulting in the formation of molecular oxygen and hydrogen peroxide.[4] The overall reaction of superoxide is catalyzed by the enzyme superoxide dismutase.

Superoxide dismutases (SODs) contain metal cofactors, which catalyze the reaction as shown below in Equation 3A and 3B.[5]

$$M^{n+} + O_2^{\cdot -} \rightarrow M^{(n-1)+} + O_2 \qquad (3A)$$

$$M^{(n-1)+} + O_2^{\cdot -} + 2H^+ \rightarrow M^{n+} + H_2O_2 \qquad (3B)$$

The reaction of superoxide catalyzed by SOD prevents oxidative stress, as superoxide would otherwise form the hydroxyl radical, which is cytotoxic.[2] The SOD reaction has a rate constant of 5 x 10^{11} $M^{-1}s^{-1}$, showing that this enzyme has extremely high activity, making it extremely efficient at converting superoxide to hydrogen peroxide and important to cell survival.[6]

1.C. Targeting Superoxide Dismutase

Superoxide is generated by antibiotics to induce oxidative stress in bacterial cells. Kohanski et al. showed that bactericidal antibiotics kill bacterial cells through the production of hydroxyl radials from superoxide via the Fenton Reaction.[7] One possible way to increase antibiotic efficacy is to interfere in the processes that protect cells from superoxide and the hydroxyl radical.[7] Inhibiting superoxide dismutase would increase the bacteria's sensitivity to these reactive oxygen species,[8] making it easier to kill the cell. SOD is critical to oxidation-reduction potential balance and is implicated in many diseases from cancers[8] and Amyotrophic Lateral Sclerosis[9] to malaria[10] and tuberculosis.[7] For this reason, there has been a call for the development of SOD inhibitors as drugs.

Recent research shows that superoxide dismutase inhibitors have potential as drugs. In 2000, Huang et al. examined the use of oestrogen derivatives as inhibitors of SOD in leukemia cells.[8] They determined that 2-methoxyestradiol selectively inhibited

human SOD, killing leukemia cells while preserving the healthy lymphocytes. The inhibition of SODs resulted in free-radical damage of mitochrondial membranes, releasing cytochrome c and causing apoptosis.[8] This result shows that one can inhibit SOD, cause oxidative stress and ultimately kill cells selectively. Other known inhibitors are metal chelating agents[11] such as diethyldithiocarbamate[12] and small anions such as azide, cyanide and hydroxide that compete for the enzyme's active site.[8] These inhibitors are poor drug candidates as they are non-specific and potentially cytotoxic.[8]

1.D. SOD Assays

High throughput SOD assays have to be used to screen libraries of molecules for inhibition. Using the natural substrate, superoxide, as a model for selecting inhibitors is not a possibility.[10] Traditionally, the screening for SOD targets has involved the use of SOD assays, which observe superoxide reactions.[13] SOD assays involve the generation of superoxide from an enzymatic (xanthine oxidase) or non-enzymatic (NADH/PMS system) source. The generated superoxide reduces a detector molecule (NBT or ferricytochrome c) and the absorbance is measured.[13] Assays, which use an enzymatic source of superoxide, may be inaccurate for high throughput screening (HTS) as molecules could inhibit the superoxide source.[10] Soulere discovered that SOD assays that generate superoxide are not selective enough for HTS because screening compounds can affect the redox balance of the assay.[10] Compounds, which interfered with the assay, showed either apparent inhibition or 'superoxide dismutase-like' activity suggesting that superoxide reacted with library compounds.[10] This result shows that assays that do not involve superoxide generation must be used for accurate high throughput screening.

1.E. ^{19}F NMR Based Assays

^{19}F NMR assays use the fluoride anion as a superoxide mimic, where an inhibitor would compete with fluoride for the active site.[14] Viglino, et al. established the use of ^{19}F NMR as a CuZnSOD assay.[14] They measured the T_1 and T_2 relaxation rate constants of $^{19}F^-$ as a function of oxidized CuZnSOD concentration and determined that fluoride coordinates to the copper and that the rate of binding controls the T_2 relaxation rate of fluoride.[14] The relaxation of fluoride is so sensitive to the presence of CuZnSOD that 10^{-8} M concentrations can be detected.[14] Compounds that inhibit CuZnSOD (azide and cyanide) were also found to inhibit the relaxation of fluoride.[14] This shows that relaxation can be used as an indirect detector of inhibition and thus be used for compound screening.

The ^{19}F NMR assay was further developed by Summers[15] for high throughput screening of superoxide dismutase inhibitors. The relaxation rate of fluoride is sensitive to the presence of oxidized SOD[14]; therefore, 100 catalytic units per 600 μL sample can be detected with a low field strength spectrometer.[15] As shown in Figure 1A and 1B, the resonance of the internal reference, trifluoroacetate (tfa), is less sensitive to relaxation by the enzyme, while the presence of active superoxide dismutase greatly diminishes the peak intensity of the fluoride anion.[15]

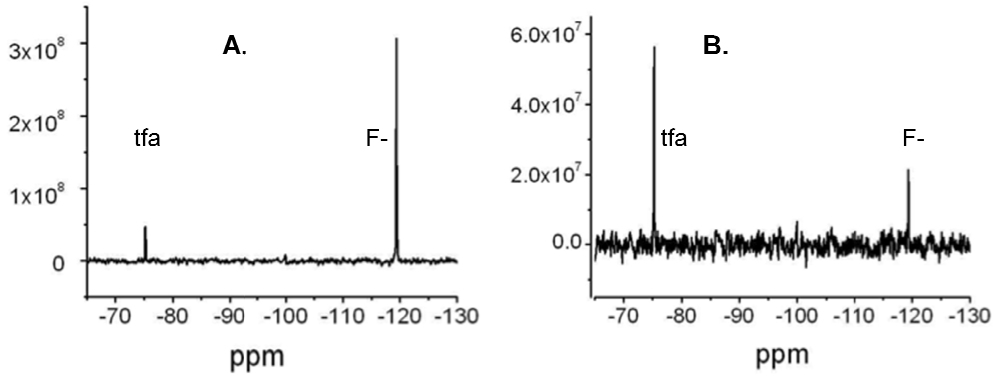

Figure 1. Effect of SOD on ^{19}F spectra. A. 1 transient CPMG spectrum of diamagnetic tfa (5 mM) and F^- (20 mM NaF) solution (40 ms relaxation). B. Effect of ~100 units Cu/Zn SOD.

Trifluoroacetate is consistently less affected by the presence of active SOD when compared to the fluoride anion. The application of pulse delay and refocusing allows time for the F^- signal to relax, enhancing of the differences between the integrals.[16] The natural logarithm of the ratio of tfa and F^- integrals [$\ln(I_{tfa}/I_{F^-})$] is directly proportional to the concentration of the enzyme as shown in Figure 2.[15]

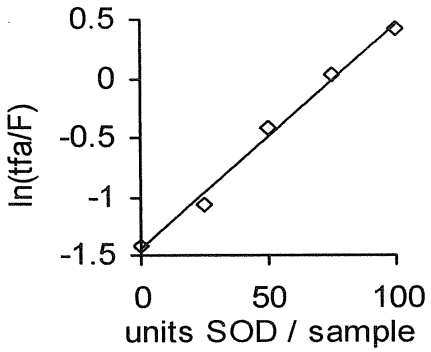

Figure 2. Ratio of tfa to fluoride ^{19}F Resonance Integrals Correlate with SOD Concentration.[15]

The concentration of active enzyme [SOD_{Ac}] can be calculated from a single measurement using Equation 4.

$$[SOD_{Ac}] = C_1 \ln \frac{I_{tfa}}{I_{F^-}} + C_2 \quad (4)$$

In which I_{tfa}/I_{F-} is the ratio of resonance integrals and the constants (C_1 and C_2) are based on the resonances' sensitivity to relaxation by the enzyme, the delay and concentrations of F^- and tfa. A benefit of using this method is the elimination of the need for shimming between samples as the loss in field homogeneity is indicated in the resonance loss of tfa.[15]

1.F. Phytoestrogen CuZnSOD Inhibition

Using the ^{19}F NMR based assay, the effect of 2-methoxyestradiol (2ME) on CuZnSOD activity was measured.[15] Huang, et al reported an inhibitory concentration of 20 μM.[8] We were unable to observe inhibition at 100 μM at neutral pH using the NMR based assay. An alternative method described by Rigo[17] using the detection of superoxide had the same result. This result was possibly caused by poor solubility of 2-methoxyestradiol at neutral pH. As Huang, et al.[8] achieved inhibition in a 50 mM carbonate solution; the pH was likely to be above 9.3 resulting in an increased solubility due to the deprotonation of the phenol proton. The experiment was repeated at pH 10.3 containing 50 mM carbonate, resulting in complete inhibition.

Since inhibition by 2-methoxyestradiol was not observed at neutral pH, we decided to look for other compounds that inhibit SOD at alkaline pH. We reasoned that the 2ME phenol group deprotonation was important and decided to look at other compounds containing phenols. Seven phytoestrogens[18] were screened for inhibition of CuZnSOD at 50 μM and pH 10.3. Of these quercetin was found to inhibit with an IC_{50} of 640 nM.[15] Quercetin only varies slightly in structure from the inactive compound

apigenin c; quercetin has hydroxyl groups at R_1 and R_2 while apigenin c does not, the overall structure shown in Figure 3.

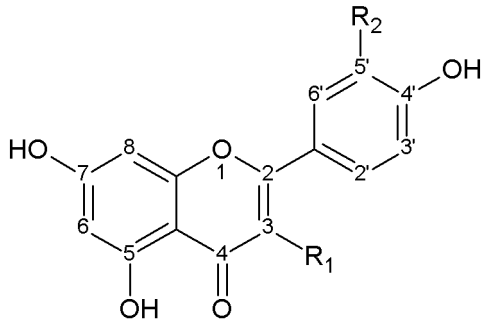

Figure 3. General Flavonol Structure.

We noted that quercetin but not apigenin inhibits CuZnSOD. These two compounds differ by the presence of alcohol groups at R_1 and R_2 in quercetin that are not present in apigenin. This observation and the binding of 2-methoxyestradiol to CuZnSOD lead our group to hypothesize that the catechol moiety on the B ring (shown in Appendix C) of quercetin may be important to binding. To further assess the role of a catechol moiety in binding, kaempferol was screened for inhibition. It was found that kaempferol inhibited at alkaline pH with an IC_{50} of 160 μM. Kaempferol was found by Sharma, et al. to increase the effect of doxorubicin (a chemotherapy agent) and increased oxidative stress causing apoptosis in glioblastoma cells.[19] These findings and research completed by our group demonstrate the potential of flavonoids as CuZnSOD inhibitors.

Described in this thesis is the inhibition of CuZnSOD by flavonol compounds. We also describe our efforts to increase throughput for screening. A main goal of this study was the development of a flavonol structure-activity relationship using ^{19}F NMR kinetic studies and docking calculations. The inhibition of ^{19}F relaxation by known CuZnSOD inhibitors, showed the ability of this assay to screen and characterize

inhibitors for SODs. High throughput screening was performed using a 500-compound library obtained from the Chemical Methodologies and Library Development Center at the University of Pittsburgh. Also, additional compounds were screened for their potential ability to inhibit. Compounds found to inhibit CuZnSOD or MnSOD have potential as anti-cancer[8] and anti-bacterial drugs.[7] Structure activity relationships can help further development of inhibitors with increased binding affinity and specificity.

2. MATERIALS AND METHODS

2.A. CuZnSOD and MnSOD Standardization

75,000 unit samples of enzymes CuZnSOD and MnSOD were obtained from MP Biomedicals LLC. Enzymes were diluted to 1mL with HPLC H_2O and 2 µL enzyme solution was removed and added to 600 µL stock NaF solution. The enzyme sample activity was determined using the CPMG[16] method (Eq. 9) and the amount of enzyme adjusted until the appropriate relaxation rate was obtained (30-100 s^{-1}). The enzyme solution was divided into portions of approximately 3000 units (40 µL) and dehydrated using centrifuge evaporation. Once the samples had been evaporated, they were placed in the freezer until needed. For inhibition studies, a portion was diluted to 200 µL with HPLC H_2O to make stock solution. 10 µL of stock CuZnSOD was added per 600 µL sample. The amount of MnSOD needed was significantly smaller than for CuZnSOD, therefore only 2-3 µL of MnSOD was needed per 600 µL NMR sample. The amount of SOD necessary to produce an appropriate relaxation rate increases with pH, and thus additional SOD was added to samples at alkaline pH.

2.B. Stock Solution Preparation

2.B.1. Sample Solution Overview

NMR solutions were prepared with sodium fluoride (NaF) and buffer in 10% deuterium oxide (D_2O). Samples for high throughput screening also contained sodium trifluoroacetate (Natfa) as an internal reference. The internal reference, Natfa, was prepared from 1:1 mole ratios of trifluoroacetic acid and NaOH at 200 mM concentrations and then diluted to 2 mM for sample stock solution. Sodium fluoride aqueous solution was prepared at 40 mM or 200 mM concentrations and was often

included in buffer solution of the same concentration. They were diluted to 20 mM for NMR studies.

2.B.2. Buffer Preparation

Buffers for pH dependence studies were prepared with pH ranging from 3 to 11.6. The buffers are listed in Table 1. For inhibitor screening at physiological pH, PIPES buffer was used. Buffers were prepared at 40 mM or 200 mM concentrations with sample solutions containing 20 mM buffer.

Table 1. Buffers Used in Sample Preparation at Various pH Values.

pH	BUFFER
3	Citric acid
3.5	2-Chloropropionoic acid
5	Sodium Acetate/Acetic acid
6-8	Pipes or HEPES
8-9	Tris
9-11	Glycine
10.5-11.5	Triethylamine
11-12	Na_2HPO_4

Citric acid, chloropropionoic acid, Na_2HPO_4 and acetate buffers were used for the pK_a determination of flavonols. An additional buffer, sodium borate ($Na_2B_4O_7$) was used to dissolve acetophenone compounds at pH 8.53. Triethylamine was prepared and used almost immediately while other buffers were stored at room temperature.

2.B.3. Preparation of Assay Controls

All experiments were conducted with a positive (SOD) control and a negative control. Negative controls contained stock solution: 20 mM NaF/buffer solution with 10% D_2O. Controls for screening also contained 2 mM Natfa. Positive (SOD) controls contained stock solution with a given amount of SOD enzyme (i.e. 10 µL of CuZnSOD per 600 µL of sample solution). This solution was vortexed and used for the positive

control and inhibitor samples were prepared so as to contain a homogeneous amount of enzyme. Controls and samples solutions were maintained at a temperature of 25 ℃ throughout experiments.

2.C. ^{19}F NMR Based Screening

In this project, we employed the NMR based assay first reported by Viglino[14] and later developed by Summers[20] to screen a large number of chemical compounds for their abilities to inhibit SODs. The assay measures the effect that the oxidized form of superoxide dismutase has on ^{19}F NMR relaxation.[15] The relaxation rate of the fluoride anion is very sensitive to SOD.[14] This allows for the determination of SOD concentration from the relaxation rate of fluoride. The one dimensional CPMG[16] method described in the introduction section 1.E. was used for the qualitative screening of molecules for SOD inhibition.

2.D. HTS Activity Determination

Screening was done using the ^{19}F NMR based assay described in the introduction section 1.E. Inhibition was determined from the ratio of the resonance integrals of tfa and F^-. As shown in Figure 1 of the introduction, the presence of active SOD increases F^- relaxation while having little effect on the relaxation of tfa. Therefore, an inhibited sample should have an increased resonance integral for F^-, yielding a smaller ratio. Compounds, which yield smaller ratios, are potential binders with complete inhibition being reflected by a return to the ratio of the negative control or an almost complete restoration of enzyme activity. The enzyme activity was determined according to Equation 5 from the ratio of resonance integrals (I) for tfa and F^-.

$$Activity = \frac{\ln(\frac{I_{tfa}}{I_{F^-}})_{Sample} - \ln(\frac{I_{tfa}}{I_{F^-}})_{NegControl}}{\ln(\frac{I_{tfa}}{I_{F^-}})_{SODcontrol} - \ln(\frac{I_{tfa}}{I_{F^-}})_{NegControl}} \quad (5)$$

Compounds, which showed some decrease in activity, were rescreened.

2.E. CPMG Pulse Sequence

Inhibitors were characterized using ^{19}F NMR and the CPMG[16] pulse sequence equipped on the JEOL Eclipse 300 NMR at Western Carolina University. The CPMG pulse sequence consists of a 90° pulse followed by a delay of τ, then a 180° pulse followed by a delay of 2τ and another 180° pulse.[16] After time τ, the nucleus is in the y-axis and the signal is observed in the y-direction from time 4τ to 40τ, observing the signal decay with time.[16] The integral (I) of each signal at time (t), where $t = 4\tau, 8\tau...$ 40τ, can be described by Equation 6.

$$I = I_0 e^{-R_2 t} \quad (6)$$

Equation 6 relates the signal integral (I) to the relaxation rate (R_2), which describes how the signal decays with time. Origin was used to integrate the signal at time t and determine the relaxation rate, according to Equation 7.

$$\ln(I) = \ln(I_0) - R_2 t \quad (7)$$

$$R_2 = k[SOD_{Ac}] \quad (8)$$

Where the relaxation rate (R_2) is determined from the linear change in the resonance integral (I) with time, t. Since the relaxation rate is directly related to active enzyme concentration, as shown in Equation 8, the CPMG method can be used to accurately measure the active SOD concentration and SOD activity.[16] The R_2 values were used to determine the CuZnSOD activity of each sample as shown in Equation 9.

$$Activity = \frac{R_{2,Sample} - R_{2,NegControl}}{R_{2,SODcontrol} - R_{2,NegControl}} \quad (9)$$

R_2 values from this method were used to determine activity for inhibitor kinetics studies.

2.F. Enzyme Inhibition Kinetics

The CuZnSOD inhibition kinetics were characterized for flavonol compounds and 9-anthracenecarboxylic acid. Observed rate constants (k_{obs}) were determined at alkaline pH for flavonols and apparent rate constants (k_{app}) across pH range 7 to 10.9 for ACA. Observed rate constants are determined from apparent rate constants as shown in Equation 10.

$$k_{obs} = \frac{k_{app}}{[Inh]} \quad (10)$$

Where [*Inh*] is the flavonol inhibitor concentration and k_{app} is determined below, according to Equation 11A and 11B. Activity was measured using either the screening method (Eq. 5) or the CPMG method (Eq. 9). The activity was observed to decay exponentially with time as shown in Equation 11A. Plots of the logarithm of the activity versus time were linear as shown in Equation 11B.

$$A = A_0 e^{-k_{app} t} \quad (11A)$$

$$\ln A = {}^{-}k_{app} t + \ln A_0 \quad (11B)$$

Where *A* is the activity determined from the NMR study over time and A_0 is the initial activity of enzyme determined from y-intercepts of plots of log *A* versus time. We expected that A_0 would equal the activity of the enzyme in the absence of inhibitor or would equal the activity of the control. We observed, however that A_0 was significantly less than the activity of the control. We attribute the difference to an initial equilibrium

step that results in less than 100% initial activity at *t*=0. This initial inhibition step can be characterized by the dissociation constant K_d as shown in Equation 12A and 12B.

$$SOD_{Ac} + Inh \underset{K_d}{\longleftrightarrow} SOD_{InAc} \quad (12A)$$

$$K_d = \frac{[SOD_{Ac}][Inh]}{[SOD_{InAc}]} \quad (12B)$$

Where [SOD_{Ac}] is the concentration of active SOD, [SOD_{InAc}] is the inactive or inhibited SOD concentration, and [*Inh*] is the monomeric inhibitor concentration. If $\%SOD_{Ac}$ + $\%SOD_{InAc} = 100\%SOD$, the K_d can be re-written in terms of active SOD ($\%SOD_{Ac}$) as shown in Equation 13A. The dissociation constant is inversely related to 1/$\%SOD_{Ac}$ -1 as shown below in Equation 13B.

$$K_d = \frac{\%SOD_{Ac}}{1-\%SOD_{Ac}}[Inh] \quad (13A)$$

$$\frac{[Inh]}{K_d} = \frac{1}{\%SOD_{Ac}} - 1 \quad (13B)$$

K_d values were determined for myricetin, morin and 2,4,6-trihydroxyacetophenone from the relationship between initial activity (A_0) and the concentration of inhibitor ([*Inh*]). The relationship between initial activity ((1/A_0)-1) and inhibitor concentration [*Inh*] was not linear for flavonol compounds, myricetin and morin. We believe this was due to aggregation of the flavonols above certain concentrations. Maximum K_d values were obtained from the initial linear relationship between initial activity and flavonol concentration. The dissociation constant is defined where the concentration of inhibitor [*Inh*] refers to the monomeric concentration only. Flavonol concentrations may actually be less than experimentally measured, as flavonol molecules may not be in monomeric form because of aggregation. Larger forms do not inhibit the enzyme; therefore, as aggregation occurs and the concentration of the

monomer decreases, the dissociation constant decreases. For this reason, reported dissociation constants are observed maximum values not best fit values.

The dimerization of flavonol inhibitors can be described by Equation 14A with a dimerization constant (K_{dim}) shown in Equation 14B.

$$Inh + Inh \xleftrightarrow{K_{\dim}} Inh_2 \qquad (14A)$$

$$K_{\dim} = \frac{[Inh_2]}{[Inh]^2} = \frac{[Inh_{tot}] - [Inh]}{2[Inh]^2} \qquad (14B)$$

Where [Inh_{tot}] is the total (experimental) inhibitor concentration and [*Inh*] is the total monomeric inhibitor concentration. The dimerization constant determines the actual concentration of monomeric inhibitor [*Inh*], which is the active species that inhibits SOD. The monomeric inhibitor concentration [*Inh*] is related to the total inhibitor concentration by the quadratic equation shown in Equation 15.

$$[Inh] = \frac{-1 + \sqrt{1 + 8K_{\dim}[Inh_{tot}]}}{4K_{\dim}} \qquad (15)$$

The best fit of the K_d and K_{dim} values to the data was calculated from the difference between calculated and experimental values of ($1/A_0$)-1 using least squares analysis.

2.G. pH Dependence of Inhibition Kinetics

The inhibition of CuZnSOD by 9-anthracencecarboxylic acid (ACA) was studied across the pH range 7 to 11.6. The apparent rate constant (k_{app}) was measured for the 1mM ACA inhibition of CuZnSOD from pH 7 to 11.6 using the CPMG method. Activity was determined using R_2 values (Eq. 9), and the apparent rate constants calculated (Eq.11B). The relationship between pH and the apparent rate constant was fitted with a pH titration curve and the pK_a estimated.

2.H. Aggregation Experiments

Using UV-Vis spectroscopy, the effect of concentration on absorbance was measured for myricetin and kaempferol. Samples were prepared with varying concentrations of flavonol in a solution of 20 mM buffer and NaF. Flavonols were dissolved in DMSO at 50 times the sample concentration so that the addition of 20 µL flavonol to 1 mL of 20 mM buffer/NaF solution would yield an overall concentration of 2% DMSO. Blanks were prepared in a similar manner with the addition of DMSO in lieu of flavonol solution to yield 2% DMSO sample solution. Kaempferol samples contained 11.6, 23.3, 46.5, 93, 186 µM concentrations of flavonol and were prepared with PIPES buffer at pH 7.94. For the initial myricetin experiment, the samples contained 3.1, 6.2,12.3, 24.6, 36.9, 49.3 µM concentrations of myricetin with the same buffer used in the kaempferol experiment. Absorbance was measured using a Hewlett-Packard model 8453 UV-Vis spectrometer with a 1 centimeter quartz cuvette.

Kaempferol and myricetin were the only flavonols examined in this aggregation study. However, all flavonols are structurally similar and are likely to aggregate. At pH 7.94, a Beer's law plot was generated for kaempferol at 274 and 382 nm. A Beer's Law plot was not generated for myricetin because the absorbance was greater than 2.5 absorbance units for 3 µM to 50 µM myricetin. The experiment was repeated using a SpectraMax microplate reader because it uses a smaller pathlength, allowing us to measure absorbance without decreasing the sample concentration. Samples were read vertically instead of horizontally, therefore the pathlength was determined by the volume of the sample instead of the dimensions of the cuvette. 100 µL samples were measured in triplicate in a quartz SpectraPlate #R8024, which is usable down to 190 nm. The resulting absorbance at 220 nm was compared to the initial activity from the NMR study in the same concentration range.

2.I. High Throughput Screening

2.I.1. Compound Preparation

500 compounds were obtained from the Chemical Methodologies and Library Development Center at the University of Pittsburgh for a proof of concept study of high throughput screening. The average mass of the compounds was 400 g/mole and each had a mass of 0.5 mg. Compounds were diluted to 2.5 mM in 500 µL dimethylsulfoxide (DMSO) solution. 50 µL portions were sent in well plates to the Bruker BioSpin Corporation for high throughput screening and the remaining 450 µL portions frozen. 12.5 µL portions of the 2.5 mM compounds were added to 600 µL samples to yield 50 µM samples in 2% DMSO solution.

2.I.2. Bruker Sample Preparation and CuZnSOD Screening

Sample solution was prepared at 10 times the sample (10X) concentrations at pH 7.16 using PIPES buffer. Positive (SOD) and negative controls were prepared from stock solution. CuZnSOD enzyme was prepared by combining 25 standardized JSJM1 SOD portions so that 5 - 1 mL enzyme portions contained enough enzyme solution for 500 samples of 10 µL each. The enzyme was solution was evaporated for shipping. The 10X stock solution, controls, and enzyme were sent along with 500-50 µL portioned compounds in DMSO solution to be analyzed on an NMR equipped with a SampleJet sample changer (Bruker BioSpin, Inc.). Amy Freund of the Bruker BioSpin Corporation completed the sample preparation and analysis, which included the dilution of samples with 10% D_2O and the addition of CuZnSOD and compounds. All inhibitor screening was completed using the ^{19}F NMR based assay and inhibition determined from tfa and F^- resonance integral ratios.

2.I.3. CuZnSOD Rescreening and MnSOD Screening

CuZnSOD samples were rescreened on the JEOL Eclipse 300 NMR at Western Carolina University. Compounds showing reduced activity were re-prepared and screened. The same 500 compounds were also screened for inhibition of MnSOD. To decrease the amount of stock solution and enzyme needed for screening, the compounds were screened five at a time. This was done by combining 12.5 µL portions of 5 different compounds into a single well in a plate. They were then vortexed using a microplate mixer yielding a solution of 5 compounds at 500 µM each. 12 µL portions of the 125 5-compound solutions were added to 600 µL MnSOD samples and screened. 500-12.5 µM compounds were screened in 125 samples in approximately two hours, at a rate of approximately 5 compounds per minute.

2.J. Selective Inhibitor Screening

2.J.1. Flavonol Screening

Flavonol molecules were screened against CuZnSOD using the ^{19}F NMR based assay. Samples were prepared with stock solution containing 20 mM NaF, 2 mM Natfa, 10% D_2O and 20 mM glycine buffer at pH 10.59. Flavonols were dissolved in DMSO to yield 2.5 mM solution and diluted for 2% DMSO samples. Taxifolin, morin, galangin and kaempferol were screened at 50 µM while fisetin and quercetin were screened at 10 µM and 5 µM respectively. The activity was measured from the tfa and F^- resonance integrals (Eq. 5) and observed rate constants determined (Eq. 10).

2.J.2. Benzoic Acid, Diketone, and Chalcone Screening

Using the ^{19}F NMR screening method, benzoic and boronic acids and pyridines were screened for SOD inhibition. Stock solution was prepared with 20 mM buffer/NaF, 2 mM tfa (internal reference) and 10% D_2O. Compounds were dissolved in DMSO. The boronic and benzoic acids and pyridine compounds listed in Table 2 were screened for inhibition of CuZnSOD at 1 mM and pH 10.59 with glycine buffer.

Table 2. Compounds Screened for Inhibition of CuZnSOD at 1 mM and pH 10.59.

BENZOIC ACIDS	BORONIC ACIDS	PYRIDINES
Benzoic acid	4-carboxyphenyl boronic acid	Picolinic acid
2,4-dihydroxybenzoic acid	4-formylphenyl boronic acid	Nicotinic acid
Allyl ether of benzoic acid	8-quinoline boronic acid	
9-anthracenecarboxylic acid	5-isoquinoline boronic acid	
5-nitroisophthalic acid		

9-anthracencecarboxylic and 2,4-dihydroxybenzoic acids were rescreened for activity at pH 7.26 using PIPES buffer. 1 mM glyoxal and 10 mM 2,4-pentanedione were screened against CuZnSOD at pH 10.44 using glycine buffer. Chalcones[21] were prepared by Professor Jack Summers and screened for MnSOD inhibition at 50 μM and pH 10.44 (structures in Appendix A). Activity was determined using the screening method (Eq. 5).

2.J.3. Acetophenone Screening

The effect of 2,4,6-trihydroxyacetophenone (THAP) and 4-hydroxyacetophenone (4HAP) on CuZnSOD activity was measured using the CPMG method. Acetophenone compounds were dissolved in 1:1 concentrations of borate buffer prepared from $Na_2B_4O_7$. Samples were prepared 1:1 from 2X acetophenone solution and 2X stock solution. The effects of THAP were determined at concentrations from 37 μM to 9 mM in 10 mM borate at pH 8.58. 4HAP was screened from 0.2 to 20 mM at pH 8.53 in 20

mM borate buffer and at pH 10.59 using TEA buffer. Activity was determined using the resulting R_2 values (Eq. 9).

2.K. Flavonol pK_a Determination

Acid dissociation constants were measured for morin, myricetin, taxifolin and galangin using UV-Vis spectroscopy. Solutions contained 20 mM NaF, 20 mM buffer solution, and 50 µM concentrations of the respective flavonol. Buffers from Table 1 were used to make samples across the pH range 3 to 11.6 for each flavonol. Absorbance was measured using a Hewlett Packard model 8453 UV-Vis spectrometer with a quartz 1-centimeter pathlength. For morin, myricetin and taxifolin, pK_a values were estimated using Excel by plotting the absorbance at wavelengths 351 and 391, 370 and 322, and 288 and 326 nm, respectively. Professor Scott Huffman determined galangin pK_a values.

2.L. Mass Spectrometry of Quercetin Inhibited CuZnSOD

Quercetin and enzyme samples were prepared for analysis by mass spectrometry. Samples contained CuZnSOD and 20mM ammonium acetate buffer (NH_4OH/NH_4OAc) at pH 10.05 and did not contain NaF or Natfa. Quercetin was prepared by dissolving 0.0298 grams of quercetin in 1 mL DMSO, followed by a dilution to 2.46 mM. Enzyme solution was prepared by combining two portions (6000 units) of standardized CuZnSOD in 200 µL HPLC H_2O. The effect of ammonium acetate buffer on enzyme activity was measured by adding 5 µL portions of SOD to 600 µL NMR stock solution containing 20 mM NaF, 20 mM ammonium acetate buffer and 10% D_2O. The activity was determined using the CPMG method.

The remaining portion of CuZnSOD was divided into two portions and each diluted to 500 µL with 20 mM ammonium acetate buffer. 10 µL of 2.46 mM quercetin was added to one of the 500 µL CuZnSOD samples to yield 49.3 µM quercetin in 2% DMSO solution. The activity was measured for both samples over a two-day period in order to observe the complete decrease in activity for the quercetin-CuZnSOD sample and to make sure the activity did not decrease after the dehydration of the CuZnSOD sample. The remaining 450 µL sample solutions were dehydrated and kept frozen until samples were ready for analysis. Michael Samuel at Wake Forest University ran both samples under direct infusion with trapping column and then backwashed the sample to the QTOF mass spectrometer. Initial samples were prepared in a similar manner by Professor Jack Summers and ran by Professor David Evanoff on the Thermo LTQ Mass Spectrometer at Western Carolina University.

2.M. Docking Calculations

2.M.1. eHiTS Docking Calculations

Initial calculations were performed using the eHiTS docking program but it was found to be insufficient and results for which are not reported in this thesis. CuZnSOD and ZndefSOD active site models were constructed in Sprout from pdb files 1PU0[22] and 2R27,[9] respectively. The CuZnSOD model was docked in eHiTS version 5.9 (SymBioSys, Inc.) using tautomeric forms of the known inhibitors quercetin and kaempferol. Initial results showed the inhibitors binding outside of the active site. A dummy ligand (cyclopentane) was then inserted into the active site to indicate the preferred binding region. Despite, this modification, eHiTS did not produce meaningful results. Likely because eHiTS does not account for flexible side chains and arginine and lysine side chains were observed to obstruct the active site suggesting that flexible

residues affect access to and shape of the CuZnSOD active site. To accommodate for flexibility, definitive docking calculations have been performed using AutoDock 4.0.[23]

2.M.2. Ligand Preparation

Molecular models of 2,4,6-trihydroxyacetophenone, 2,4-dihydroxyacetophenone, apigenin, kaempferol, myricetin, quercetin and taxifolin were prepared in all of their physiologically meaningful tautomeric and protonation states. Musialik determined protonation states and acid dissociation constants of flavonoids from their structure affinity relationships.[24] From the available pK_a values of flavonols, three protonation states are expected at pH 8.

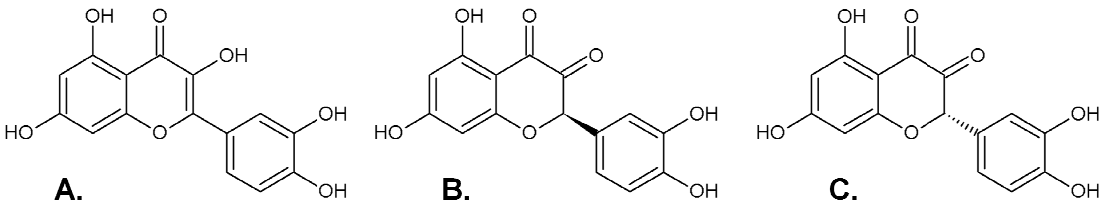

Figure 4. Tautomers of Quercetin: Enol (A), R-diketone (B), and S-diketone (C) species.

Initial conformations and partial atomic charges were generated using the 'equilibrium conformer' utility in Spartan '04 with a semi-empirical AM1 Hamiltonian.[25] In some cases, convergence problems were addressed by reducing the gradient tolerance to 3 au.[26] Ligand structures were then saved using the Tripos mol2 format with charges included. These files were then converted to the default AutoDock pdbqt format, which adds a specification as to which torsions are to be considered flexible in the docking calculations. By default, all rotable torsions were set to flexible.

2.M.3. Receptor File Preparation

The receptor file, 1PU0[22] for wild-type human SOD, was downloaded from Brookhaven and edited to monomeric form without the active site Zn and Cu ligands. This protein model spawned errors in AutoDock due to slight angular inaccuracies in the disulphide bridges. To correct this problem, we used the Anneal program in Sybyl[27] to conduct a localized minimization on all disulphide bridges, using the TRIPOS force field without electrostatics. Next, electrostatic and Van der Waals parameters for the copper and zinc cofactors were added to the AutoDock 'parameters.dat' file so that the docking calculations could take into account the potential influence of these highly charged atoms.

To ensure the most accurate electrostatic representation of the SOD, protonation states of ionizable residues and overall partial atomic charges were calculated at pH 8 using the finite-difference Poisson-Boltzmann solver in PDB2PQR[28] web server courtesy of Dolinsky, et al. The resulting pqr file was parsed into two files: one file describing the rigid part of the binding site and the other describing the flexible part of the site; ('rigid' and 'flex' pdbqt files, respectively) using AutoDockTools.[29] Flexible residues specified in the flex file are: Lys122, Lys 136, Thr137, and Arg143. The rigid file was generated with 60 x 60 x 50 Å grid centered around the active site copper. Metal cofactors were edited back into the rigid receptor file as PDB2PQR[28] does not recognize copper and zinc cofactors. Docking calculations were performed using AutoDock 4.0[23] on MAC OS X for preliminary calculations and subsequent calculations were performed on a 4 dual-core CPU Linux workstation.

2.M.4. AutoDock Analysis

Results from AutoDock were examined by comparing the energies and distances of various poses for each ligand and then ligands were compared between compounds. A pose is the conformation of the ligand in the receptor active site and the confirmation of the specified flexible amino acid residues. Poses are calculated by AutoDock and have binding energies associated with them. Distance constraints were applied so that a pose with an average distance greater than 10 Å from Arg143 was not considered. Arginine 143 is in the center of the active site and a ligand this far from the active site is not likely to represent a physically realistic binding pose. The distances between the guanidinium carbon of arginine 143 and the 7-position oxygen and the 3-position carbon were measured using the measureDistanceGC tool in AutoDockTools.[29] These specific flavonol positions were chosen because the 7-position oxygen is the site of the first deprotonation and the 3-position carbon is the site of tautomerization.[24]

Once unrealistic poses were ruled out, the top five binding poses for each species of each ligand was plotted as a function of the logarithm of experimental dissociation constants, K_d[30] for each protonation state. Trends between species and dissociation constant were observed to gain a global understanding of what species of ligand is/are likely to bind. This approach revealed that bis-deprotonated ligands are likely the binding species. Individual bis-deprotonated poses were studied to gain an understanding of what types of interactions occurred for a specific ligand. Understanding the interactions for each ligand can explain why some flavonols are stronger binders than others. It can also show what ligands have in common in terms of interactions to predict what functionality is necessary for flavonol binding. For this analysis, acetophenones were not considered, as they are structurally different enough

for it to be inappropriate to include them in the development of the structure affinity relationship for flavonols.

To observe global trends in binding energies; individual poses exhibiting specific interactions with a given residue or a ligand functional group were plotted as a function of $\log K_d$[30] for each ligand. A correlation between experimental and predicted binding energy of these poses helps uncover what functional groups and residues may be important for binding. Our experimental design was put in place to help determine what state of our ligands are most likely to bind, while specific trend analysis of individual ligands predicts why differences in binding exists and final global analysis predicts what groups and residues are involved in binding. The combination of these three analyses guides the prediction of the structure activity relationship, which can be used to guide the development of new inhibitors and optimize inhibition.

3. RESULTS AND DISCUSSION

3.A. Flavonol Inhibitor Screening

3.A.1 Flavonol Observed Rate Constants

Several flavonol molecules were screened for inhibition of the CuZnSOD enzyme at alkaline pH. The observed rate constants (k_{obs}) of each were determined and are reported in Table 3.

Table 3. Observed Rate Constants for Various Flavonols at pH 10.59

Structure	Compound	k_{obs} ($\mu M^{-1}s^{-1}$)
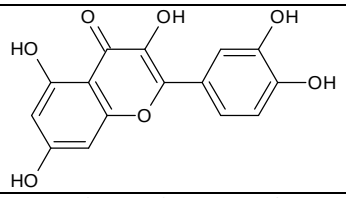	Quercetin	5.2×10^{-4}
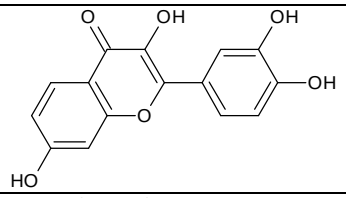	Fisetin	4.6×10^{-4}
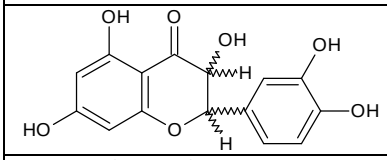	+/- Taxifolin	1.2×10^{-4}
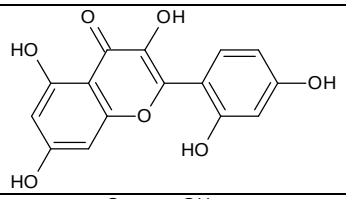	Morin	1.18×10^{-4}
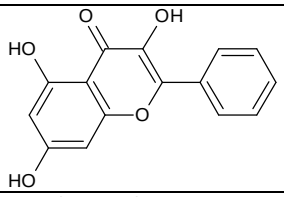	Galangin	1.04×10^{-4}
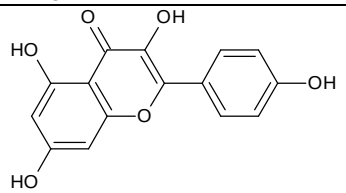	Kaempferol	6.6×10^{-5}

The observed rate constants reported in Table 3 show what structural features influence inhibition. When comparing the observed rate constant and structure of quercetin to that of other the inhibitors, the following inferences can be made. Inhibition is not caused by interactions with the 5-hydroxyl group. This is suggested by comparative k_{obs} values for fisetin and quercetin when the 5-hydroxyl group has been removed in the former. What did seem influential on the inhibition of CuZnSOD are the substituents on the B ring (shown in Appendix C). The removal of the 5'-hydroxyl group results in decreased inhibition for kaempferol and galangin. The movement of the hydroxyl group from the 5' to 6' position in morin also decreases the inhibition constant.

3.A.2. Arginine Modification

We hypothesized that inhibition could involve arginine modification. It was found that apigenin did not inhibit CuZnSOD while quercetin inhibited quickly at alkaline pH. Kaempferol, an intermediate between quercetin and apigenin, inhibits the enzyme though not as well as quercetin, suggesting that the 3-hydroxyl group is necessary for inhibition. The enol may be necessary for inhibition because it can tautomerize to the diketone moiety, which may be necessary for the inhibitor's activity. If this is true, the diketone may react according to the reaction in Figure 5, reported by Gilbert and O'Leary.[31]

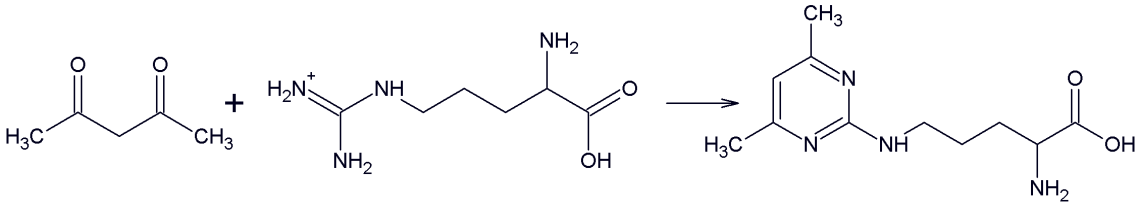

Figure 5. Reaction of 2,4-Pentanedione with Arginine forms N-substituted 2-amino-4,6-dimethylpyrimidine.[31]

In the reaction of arginine with 2,4-pentanedione, Gilbert and O'Leary found that the diketone of 2,4-pentanedione reacted with the guanidinium moiety of the arginine to form a pyrimidine ring with N-substituted 2-amino-4,6-dimethylpyrimidine being the only product.[31] Further evidence of CuZnSOD inhibition by arginine modification is the modification by p-hydroxylphenylglyoxal resulting in the deactivation of bovine pancreatic ribonuclease A as reported by Yamasaki[32] and the reaction of 1,2-cyclopentanedione with arginine to form DHCH-arginine[33] reported by Smith.[34] If such a mechanism is present, the diketone moiety of the flavonol tautomer may react with the active site residue arginine 143, an important residue for CuZnSOD function.[5]

3.A.3. 2,4-Pentanedione and Glyoxal Screening

To test this hypothesis, both 2,4-pentanedione and glyoxal were screened for inhibition. It was found that 10 mM 2,4-pentanedione did not inhibit the enzyme at pH 10.44 while 1 mM glyoxal did. Further characterization of inhibition by glyoxal was performed by Jonathan Markley. As 2,4-pentanedione does not inhibit the enzyme, inhibition of CuZnSOD cannot be by the reaction shown in Figure 5. However, the diketone in 2,4-pentanedione has an additional carbon compared to the diketone moiety of the flavonol inhibitors; therefore, modification of arginine residues cannot be completely rejected as a means of inhibition by this result alone.

3.A.4. Diketone Tautomerization

To test the diketone hypothesis, we screened taxifolin for inhibition at 50 μM and determined the observed rate constant as shown previously in Table 3. The structure of taxifolin differs from that of quercetin by reduction of the 2-3 double bond. This difference in structure results in two structural differences: taxifolin is unable to

tautomerize to the diketone form and a new chiral center is formed. The results in Table 3 show that taxifolin inhibits, although less effectively than quercetin. The inhibition of CuZnSOD by taxifolin shows that the diketone moiety is not necessary for inhibition. This result suggests that inhibition does not occur due to reactions with arginine and a diketone. This helps refute the hypothesis that inhibition occurs through arginine modification by a diketone similar to the reaction reported by Gilbert and O'Leary.[31]

Although inhibition of CuZnSOD does not occur due to arginine modification, the effect of tautomerism on molecular shape may still play a role in the increased effectiveness of quercetin as compared to luteolin. Luteolin inhibition was examined by Jonathan Markley because it also lacks the ability to tautomerize and has only one isomer whereas taxifolin has four. In luteolin, the removal of the 3-hydroxyl group, results in a lower K_d of 830 μM[30] and renders it unable to tautomerize. Taxifolin has sp^3 hybridization at the 2-carbon while luteolin and quercetin are planar due to sp^2 hybridization. To determine the contribution of sp^3 hybridization to binding, eriodictyol was screened for inhibition by Erin Parris and Corey Harrington as it is similar in structure to luteolin (structure given in Appendix D). This compound was found to only inhibit partially at high concentration and pH 8.5. This result shows that tautomerism to give a non-planar shape of flavonols is not the origin of the difference in behavior of quercetin and luteolin.

3.B. pH Dependence of CuZnSOD Inhibition

3.B.1. Acidic Inhibitor Screening

Our group previously measured the effect 100 μM 2-methoxyestradiol (2ME) has on CuZnSOD. This compound was reported by Huang to inhibit.[8] Inhibition was only achievable after the addition of 50 μM carbonate at pH 10.3 suggesting that the

deprotonation of the molecule is necessary for inhibition. As flavonols are structurally similar to 2ME, they too should show pH dependence and this has consistently been the case. In order to understand the origin of this pH dependence, the screening for more acidic inhibitors was carried out. The boronic and benzoic acids and pyridine carboxylic acids, given in the Materials and Methods section 2.J.2., were screened for inhibition of CuZnSOD. Of these 2,4-dihydroxybenzoic acid and 9-anthracenecarboxylic acid were found to inhibit at alkaline pH.

3.B.2. Determination of Enzyme Acid Dissociation Constant

Of the compounds screened for CuZnSOD inhibition, 2,4-dihydroxybenzoic acid and 9-anthracenecarboxylic acid were found to inhibit the enzyme at alkaline pH. At pH 7.26, 9-anthracenecarboxylic acid (ACA) was found to inhibit CuZnSOD completely but slower than at alkaline pH while 2,4-dihydroxybenzoic acid only slightly decreased the enzyme's activity. ACA appears to have pH dependent activity over the pH range 7 to 10.9 and has a pK_a of 3.66;[35] therefore, the pH dependence of inhibition cannot be caused by deprotonation of the molecule but by some change in the enzyme. To further examine this, the effect of pH on the apparent rate constant was measured and the plot fitted with a standard titration curve with a pK_a of 10.1, as shown in Figure 6.

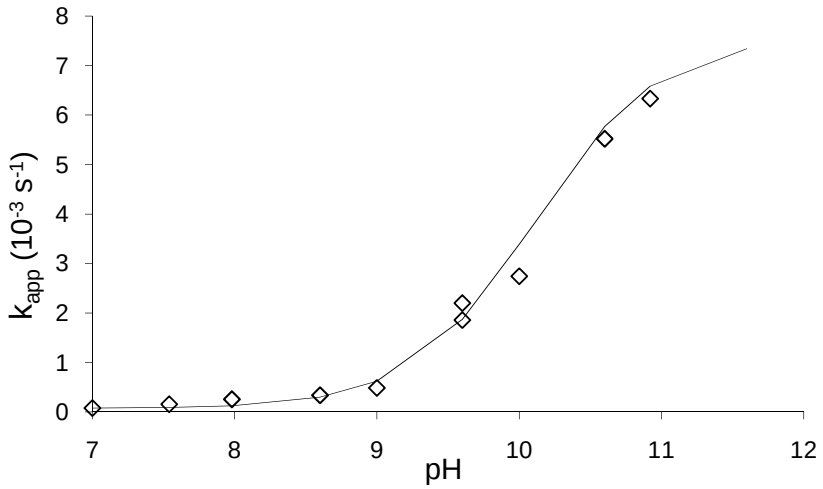

Figure 6. Effect of pH on the Apparent Rate Constant of CuZnSOD Inhibition by 1 mM 9-Anthracenecarboxylic acid.

3.B.3. Possible Enzymatic Causes of pH Dependence

The trend line in Figure 6 represents behavior predicted for an acid with an acid dissociation constant of 10.1. As the pK_a of ACA is far below this range, the deprotonation event causing pH dependence belongs to the enzyme, specifically an active site residue with a pK_a of 10.1. The active site residue lysine 122 was determined to have a pK_a of 10.1 by Argese and Viglino[36] using NMR and crystallographic data. This residue partially controls the electrostatics of the enzyme along with lysine 136.[36] This suggests that decreased enzyme activity may be caused by the deprotonation of lysine 122.[36] Another possible cause of the pH dependence of CuZnSOD is the gradual denaturation of the enzyme. However, the enzyme control sample retained activity, ruling out loss of activity due to changes in electrostatics or denaturation. Additionally, the enzyme denaturation is reported to only occur after pH 12.5.[37]

3.B.4. Replication of Enzyme Acid Dissociation Constant

The pH dependence of CuZnSOD inhibition by ACA was repeated in order to replicate the results showing an enzyme deprotonation at pH 10.1. Kinetic data was collected at pH 10.59 in order to compare the rate constant to that reported in Figure 6. This experiment resulted in an apparent rate constant (k_{app}=0.0007 s^{-1}) an order of magnitude lower than the previous experiment (k_{app}=0.0055 s^{-1}). However, this was not consistent across the pH range 7 to 11, and the determination of the acid dissociation constant was irreproducible. This may be due to the difference in the enzyme between standardized samples, which needs to be addressed in future experiments.

3.B.5. Acetophenone Screening

Using a different acidic inhibitor may yield more information about the pH dependence of the flavonol inhibition. Inhibition by acetophenones has been investigated. 2,4,6-trihydroxyacetophenone (THAP) is similar in structure to flavonol molecules as shown in Figure 7.

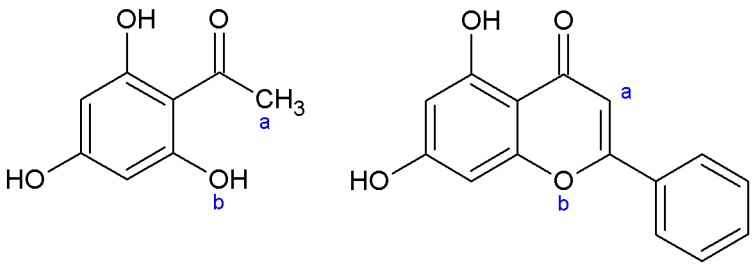

Figure 7. Structure of 2,4,6-Trihydroxyacetophenone (left) as Compared to the Flavonoid Structure (right).

The effect of THAP on initial activity is shown in Figure 8 with dissociation constant K_d of 3.5 mM at pH 8.58.

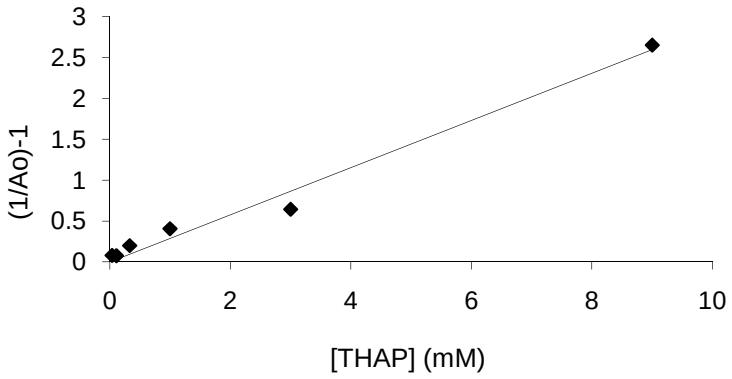

Figure 8. Inhibition of CuZnSOD by THAP at pH 8.58.

THAP was also examined for the purpose of determining the distances between the copper atom of CuZnSOD and individual protons using ^{1}H NMR experiment. These distances can be compared to computational data from AutoDock and used to help verify docking results. However, single pulse H NMR spectra show that the inhibitor is oxidizing in the air. Future experiments using acetophenones will involve using an air-free system. Another acetophenone, 4-hydroxyacetophenone (4HAP), shown in Figure 9, is less prone to oxidation and was screened for activity at pH 8.5.

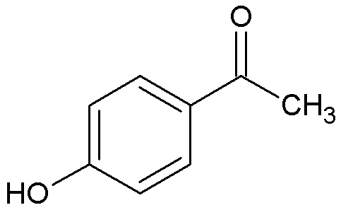

Figure 9. Structure of 4-Hydroxyacetophenone.

A concentration dependence experiment showed little change in initial activity with concentration, ranging from 0.2 to 20 mM. The compound was rescreened for inhibition at pH 10.59 for 20 mM 4HAP. The activity of the enzyme decreased from 97%

initial activity to 87% activity 21 hours later; therefore, this compound is an extremely poor binder of CuZnSOD.

3.C. Enzyme Kinetics

3.C.1. Kinetic Data Indicate Rapid Pre-Equilibrium

Upon addition of the inhibitor, it was observed that the initial activity of the enzyme was not 100%, an example of which is shown in Figure 10, where 100% activity would be indicated by a value of zero for the intercept.

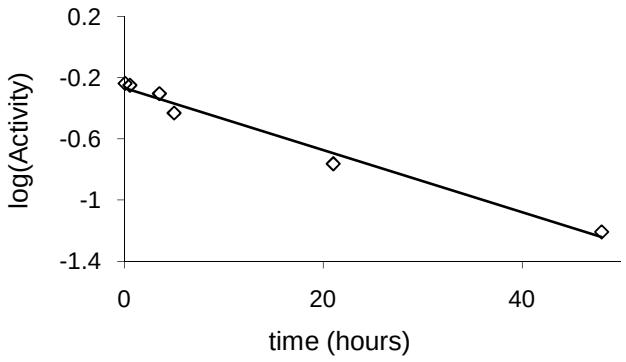

Figure 10. CuZnSOD Inhibition by 1 mM ACA at pH 8.58.

The initial loss of activity indicates an initial binding step between the enzyme and ACA. The effect of varying ACA concentration on CuZnSOD inhibition was measured at pH 8.58 from 62.5 to 1000 μM using the CPMG method. Altering inhibitor concentration changed the initial activity of the enzyme as illustrated in Figure 11. This suggests that there is a quick equilibrium inhibition reaction occurring between CuZnSOD and the inhibitor. A second inhibition step was also observed as the activity of the enzyme continues to decrease slowly over time, shown in Figure 10 above.

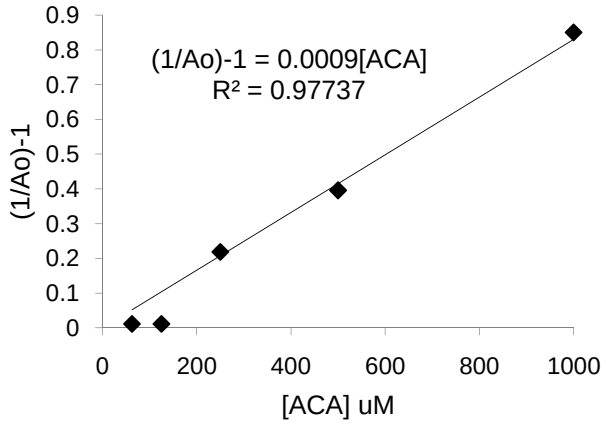

Figure 11. Concentration Dependence of Initial Activity Indicates an Equilibrium Reaction with a Dissociation Constant K_d of 1mM for ACA.

3.C.2. Effect of pH on Initial Activity

The inhibition of CuZnSOD at high pH appears to be a two-step reaction. As discussed in Section 3.B.3., the pH dependence of CuZnSOD may be caused by the deprotonation of the active site residue, lysine 122. This is not desirable in an inhibitor because it cannot be necessary to change the body's pH in order to deprotonate an enzyme and achieve inhibition. To determine of the initial binding step is affected by enzyme deprotonation, the initial activity of CuZnSOD inhibition was examined as a function of pH as shown in Figure 12.

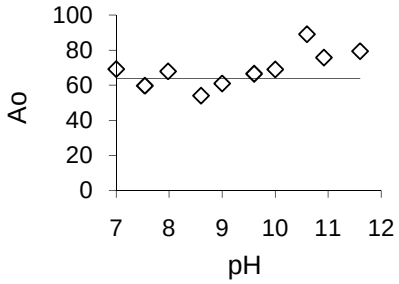

Figure 12. Effect of pH on the Initial Activity of CuZnSOD Inhibition by 1 mM ACA.

Where the initial activity, A_0 varied within uncertainty around 60% activity and is not pH dependent. We conclude that the initial binding step is pH independent. This

shows that the deprotonation of the enzyme is not necessary for binding but functions to increase the rate constant of the second slower inhibition reaction. These results lead us to propose the mechanism of inhibition in Equation 16, in which the deprotonation of the enzyme increases the rate constant, k_2 of the second step.

$$Inh + SOD_{Ac} \underset{K_d}{\longleftrightarrow} InhSOD_{InAc_1} \xrightarrow{k_2} InhSOD_{InAc_2} \qquad (16)$$

3.C.3. Effect of Flavonol Protonation State on Dissociation Constant

The protonation state of enzyme has been shown to have little effect on the initial binding of ACA. This step appears to be influenced by the protonation state of the inhibitor and therefore, can still be affected by pH. To access this possibility, the effect that pH has on the equilibrium dissociation constant K_d was measured for myricetin and morin, as shown in Table 4.

Table 4. Dissociation Constants for Myricetin and Morin.

Compound	pH	$K_{d,max}$ (μM)	pK_{a1}	pK_{a2}
Myricetin	5.48	332	6.5[15]	
	7.94	9.3		
Morin	8[30]	600	5.2[24]	8.2[24]
	8.99	408		

These pH values were selected for myricetin, as they are above and below the first acid dissociation constant for the molecule. Myricetin has a pK_{a1} value of 6.5 as determined by UV-Vis spectroscopy; the pK_{a2} value was not determined. This means that the K_d values for pH 5.48 and 7.94 correspond respectively to the binding of the protonated and singly deprotonated forms of myricetin to CuZnSOD. As a lower dissociation constant means a stronger binder, the deprotonated form of myricetin present at pH 7.94 is the

more effective binder. The same is shown for morin, as increased binding is observed above the pK_{a2} of morin, perhaps indicating that the bis-deprotonated form is more effective than that deprotonated.

3.D. pH Dependence of CuZnSOD Inhibition Considerations

When considering that both the protonation state of the inhibitor and the enzyme affect inhibition, the system becomes very complicated. Measurements of various inhibitors must be done at the same pH so as to compare inhibition against the same enzyme and not forms with varied protonation states. For this reason and to better compare flavonol inhibition results to docking results, flavonol dissociation constants K_d were re-measured at pH 8 by Jonathan Markley. These results will be discussed in context with the docking calculations in a later section.

3.E. Myricetin and Kaempferol Aggregation

As discussed in the Materials and Methods section, CuZnSOD inhibition by flavonols appears to compete with flavonol dimerization. This was first considered when the initial activity was observed to change nonlinearly with the concentration of Myricetin as shown in Figure 13.

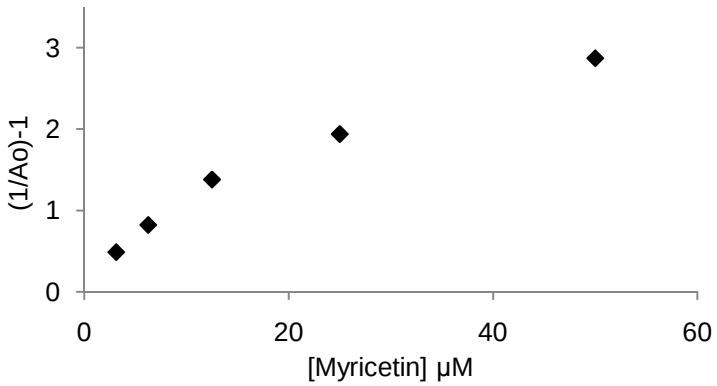

Figure 13. Initial Activity Changes Non-linearly with Myricetin Concentration at pH 7.94.

To further study aggregation, the effect of concentration on absorbance was measured for myricetin and kaempferol by UV-Vis spectroscopy. A Beer's Law plot was generated for kaempferol at pH 7.94 from 11.6 to 186 μM. As shown in Figure 14, kaempferol no longer obeyed Beer's Law above 50 μM.

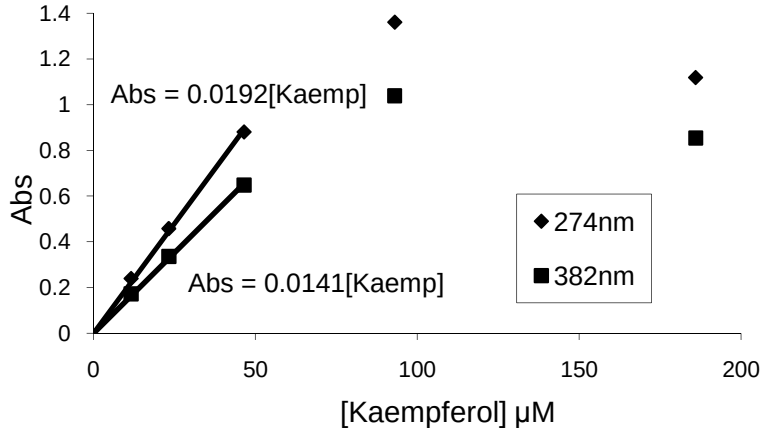

Figure 14. Beer's Law Plot of Kaempferol at pH 7.94.

For the inhibitor, myricetin, absorbance was measured from 3 to 50 μM at pH 8. A peak shift near 230nm was observed with an absorbance greater than 2.5 absorbance units with increasing concentrations from 3 to 50 μM myricetin. Since the absorbance was too high to quantify this shift using UV-Vis spectrometer, measurements were repeated using a microplate reader. Upon repeating the experiment, a nonlinear change in absorbance at 220 nm was observed and compared to the inhibition data. Figure 15 shows that both inhibition and absorbance change in the same non-linear way as the total concentration of myricetin is increased.

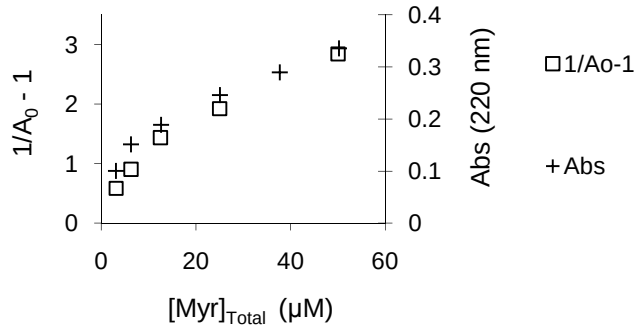

Figure 15. Concentration Dependence of Initial Activity and Absorbance for Myricetin at pH 8.

In the absence of aggregation, absorbance should correlate with concentration according to Beer's law. Figures 14 and 15 show that this is not the case. A possible explanation is that the concentration may be not increasing in a linear fashion. This would occur if the concentration of myricetin monomer were not equal to the total myricetin concentration, caused by aggregation. The increase in concentration results in a decrease in slope of the initial activity suggesting that the aggregates do not have the same effect on CuZnSOD as the myricetin monomer. This suggests that only the monomeric form of myricetin inhibits CuZnSOD while aggregates do not. Using fluorescence and UV-Vis spectroscopy, further analysis of aggregation was completed by Jonathan Markley.

Dimerization of flavonols can be characterized by a dimerization constant (K_{dim}) defined by Equations 14A and 14B, where $K_{dim} = [Inh_2]/[Inh]^2$. Using least squares analysis, the best fit of K_{dim} and K_d was calculated as described in the Materials and Methods section 2.F. In Table 5, the estimated dimerization and dissociation constants are reported for myricetin at pH 7.94 only, as the other dimerization constants were so low as to consider dimerization minimal. Other reported K_d values are maximum values discussed earlier in this thesis.

Table 5. Estimated Dimerization and Dissociation Constants for Myricetin and Morin.

Compound	pH	K_{dim} (μM^{-1})	K_d (μM)
Myricetin	5.48		332
	7.94	2.22E-01	3.3
Morin	8.99		408

As the dissociation and dimerization constants both affect the fit of the curve to the data, uncertainty in K_{dim} will cause uncertainty in K_d. For this reason, $K_{d,max}$ values are discussed instead of estimated K_d values because the experimental values are more reliable.

3.F. Determination of Flavonol Acid Dissociation Constants

UV-Vis spectroscopy was used to determine the pK_a values for myricetin, taxifolin, morin and galangin. pK_{a2} values were not determined for myricetin and taxifolin. Acid dissociation constants were later found in the literature for taxifolin and galangin. Using excel and calculations completed by Professor Scott Huffman, pK_a values were estimated, in Table 6.

Table 6. Flavonol pK_a Values Determined by UV-Vis Spectroscopy.

	pKa_1	pKa_2
Myricetin	6.5	
Taxifolin	6.7	
Morin	4.8	7.9
Galangin	7.19	9.44

3.G. High Throughput Screening

This study was conducted to show that the ^{19}F NMR based assay could be used to screen large quantities of compounds quickly. For this proof of concept experiment, 500 compounds from the Chemical Methodologies & Library Development Center at the University of Pittsburgh were screened against two targets: CuZnSOD and MnSOD at pH 7.26. Amy Freund of the Bruker BioSpin Corporation screened these compounds against CuZnSOD using a SampleJet sample changer (Bruker BioSpin, Inc). None were found to inhibit CuZnSOD.

At Western Carolina University, samples were rescreened for activity and several compounds showed marginally decreased SOD activity, suggesting that inhibition may be occurring. Re-preparation of the samples showed little change in enzyme activity. All 500 compounds were screened against MnSOD and none of these samples were found to inhibit the bacterial enzyme. Chalcones were also screened for inhibition of MnSOD at alkaline pH and none inhibited. Chalcone molecules were screened as Soulere found they inhibit FeSOD in Plasmodium falciparium and as MnSOD and FeSOD are similar in structure, it is possible a compound that inhibits one may inhibit the other.[10]

The failure to discover new inhibitors cannot be used to refute the concept of using ^{19}F NMR based assays as a method for SOD inhibitor screening. This experiment did show that the assay can be used to screen for inhibitors quickly as 500 compounds were screened in only 2 hours. If this screening method were paired with high throughput screening docking calculations, a very large library could be narrowed down and screened very quickly while increasing the chance of finding inhibitors.

3.H. Quercetin Inhibition of CuZnSOD Observed by Mass Spectrometry

In order to understand where the inhibitor quercetin is binding in the active site of CuZnSOD, active and inhibited enzyme samples were analyzed using mass spectrometry. Professor Jack Summers prepared samples of CuZnSOD and CuZnSOD inhibited with quercetin for analysis at Western Carolina University. Analysis by David Evanoff resulted in no observed molecular ion and the CuZnSOD-quercetin sample showed a decrease in viscosity as compared to the active enzyme sample. Samples were re-prepared after it had been determined that sample conditions did not affect CuZnSOD activity. Michael Samuel, using quadrupole time-of-flight mass spectrometry, analyzed them at Wake Forest University. Resulting mass spectra are shown in Figures 16A and 16B for CuZnSOD and quercetin inhibited CuZnSOD samples respectively.

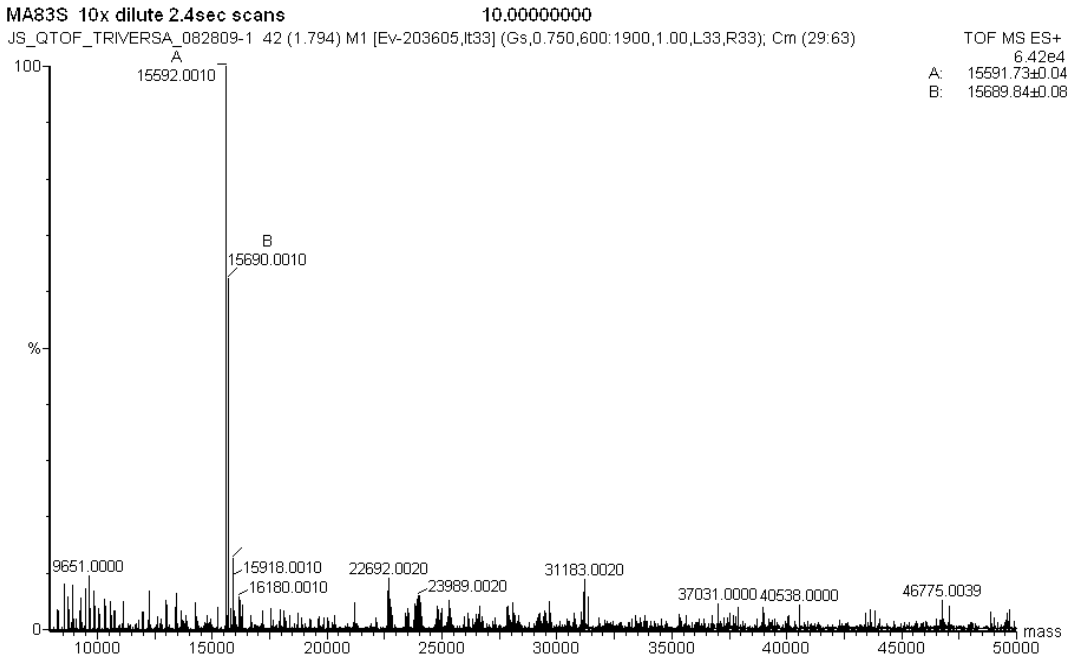

Figure 16A. Mass Spectrum of 2500 Units of Active CuZnSOD.

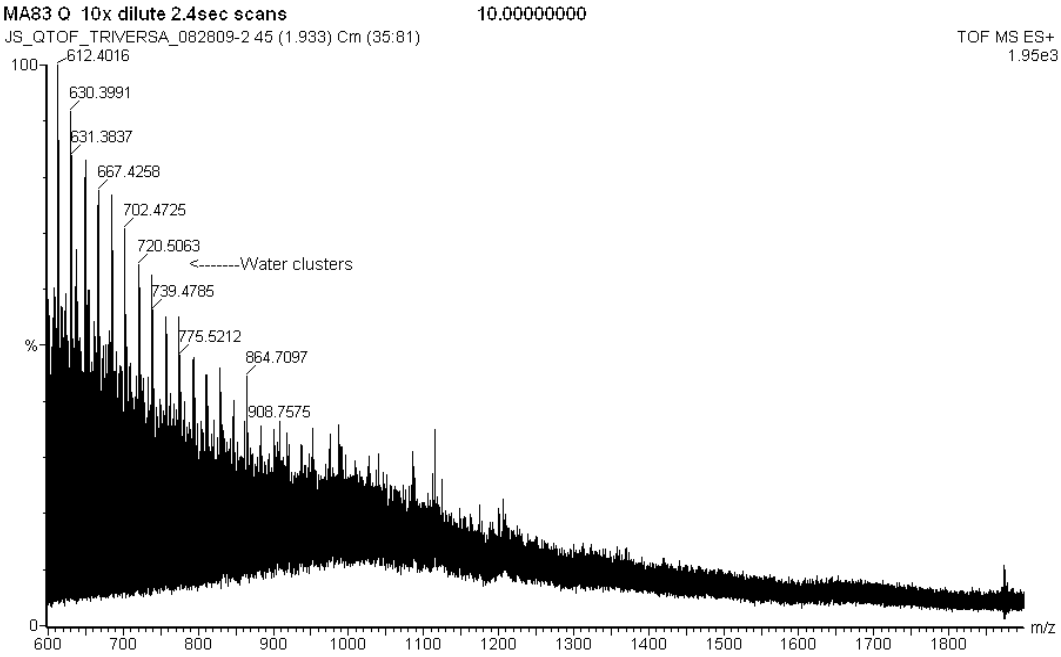

Figure 16B. Mass Spectrum of 2500 Units of CuZnSOD Inhibited with 50μM Quercetin.

Figure 16A shows mass to charge ratios as high as 50,000 while 16B only shows ratios up to 1800. As CuZnSOD has an approximate molecular weight of 32,000,[5] both samples should have peaks around 32000 for the singly charged enzyme and 16000 for the doubly charged enzyme. The mass spectrum of active CuZnSOD in Figure 16A, reflects the presence of enzyme with a molecular ion peak at 15592 and a second smaller peak at 15690. The mass spectrum of inactive CuZnSOD shown in Figure 16B, does not show this molecular ion peak nor does it show any smaller peaks which would be represent enzyme fragments. The presence of only solvent peaks suggests that no enzyme was present in the sample, even though enzyme was added to both samples in equal amounts. Since the enzyme was present in both samples, the lack of a molecular ion peak or fractions could be due to the enzyme never reaching the spectrometer. This can be explained by possible precipitation of the enzyme from solution. This hypothesis is supported by the observed decrease in viscosity in the CuZnSOD-quercetin sample as compared to the active CuZnSOD sample.

3.I. Docking Calculations

3.I.1. Global Analysis

In order to understand the inhibitor binding interactions with CuZnSOD, docking calculations were performed using AutoDock 4.0.[23] If our models are correct, then docking should predict the structure activity relationship for the binding of flavonols discussed earlier. These include lower K_d values above an inhibitor's pK_a observed for myricetin and morin (reported in Table 4) and the observed trend in K_d values at pH 8 (given in Appendix B). Based on these trends, docking calculations should predict deprotonated ligands will bind stronger than neutral ligands and compounds to bind with decreasing effectiveness in the following order: myricetin > quercetin > taxifolin > kaempferol >> apigenin > 2,4-dihydroxyacetophenone > 2,4,6-trihydroxyacetophenone. Both have been observed to be the case.

The global trend analysis shows that bis-deprotonated binding poses correlate to the experimentally determined dissociation constants as shown in Figure 17C. Figures 17A and 17B show the box charts of pose binding energies for neutral and deprotonated ligands respectively. Box and whisker plots represent the statistical variation in the binding energy of docking poses: boxes show the 25th, 50th, and 75th percentiles and whiskers, the 10th and 90th percentiles. The circles show the highest and lowest binding energies or the extrema and squares represent the average or mean binding energy.

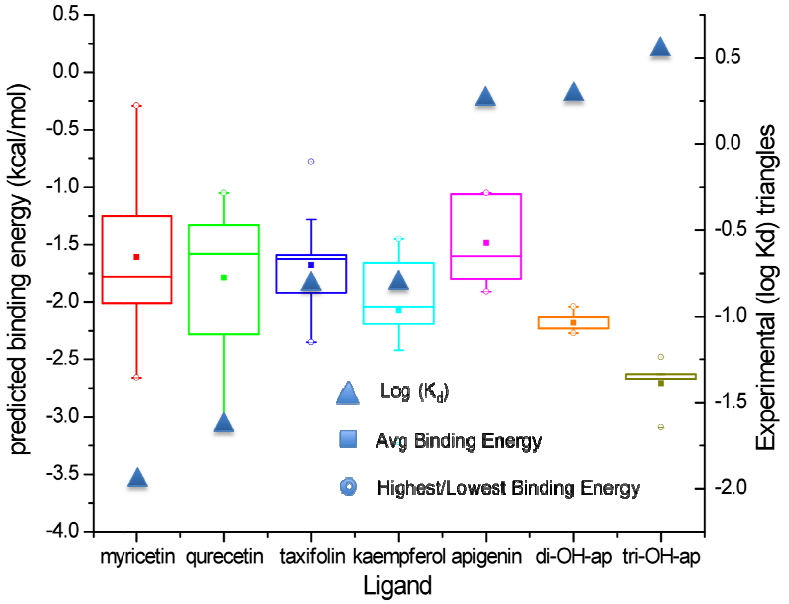

Figure 17A. Neutral Ligand Pose Binding energies do not correlate with Experimental Data. Box and whisker plots represent the statistical variation in the binding energy of docking poses: boxes show the 25th, 50th, and 75th percentiles and whiskers, the 10th and 90th percentiles. The circles show the highest and lowest binding energies or the extrema and squares represent the average or mean binding energy.

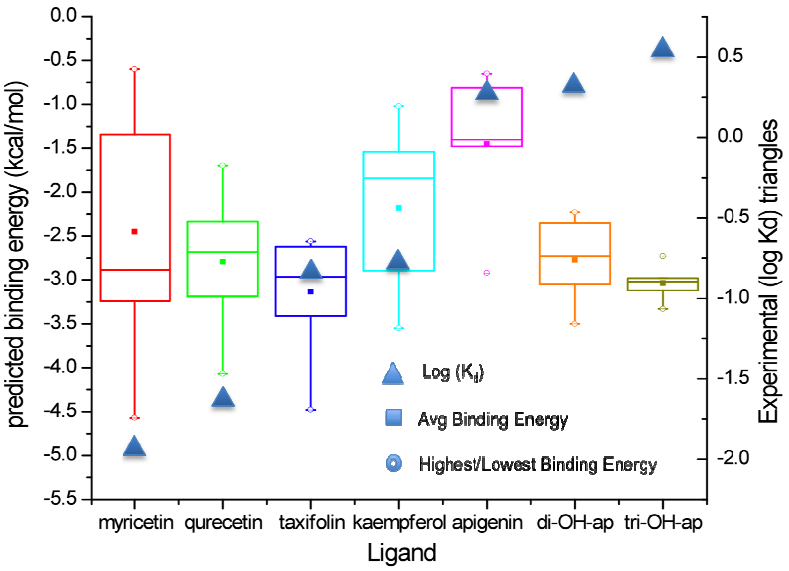

Figure 17B. Deprotonated ligand pose binding energies do not correlate with experimental binding constants.

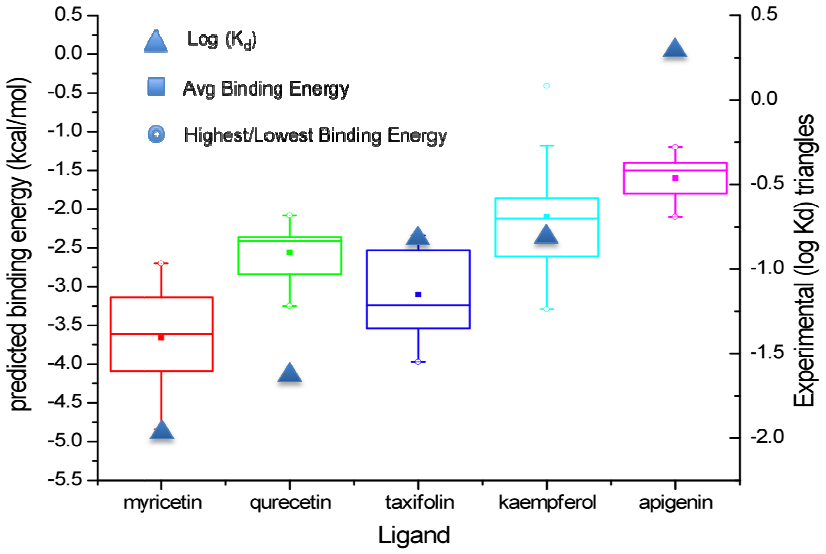

Figure 17C. Bis-deprotonated flavonols are predicted to bind favorably as pose binding energies correlate to experimentally determined dissociation constants.

Acetophenones were excluded from the trend analysis for bis-deprotonated ligands, as they are only mono-anionic. Excluding acetophenones, the global trend analysis for each protonation state still shows bis-deprotonated ligands to fit the experimental data the best. Individual poses correlating to experimental Log K_d values were enol and S-diketone tautomer species. This predicts S-enantiomers of diketone tautomers appear more likely to bind than R-enantiomers. The trend analysis also predicts apigenin to be a better binder than observed experimentally. This discrepancy could be due to inaccuracies in the model and/or errors in the experimental data.

Inaccuracies in the model can originate from shortcomings of forcefield based docking. One such inaccuracy is the inability of AutoDock 4.0[23] to account for π-Cation interactions in the docking calculation. The conjugated π system of flavonols could interact with lysine and arginine residues in the active site through such interactions; the docking calculations may not fully characterize the binding because it ignores this

possibility.[38] Other possible sources of inaccuracies include the exclusion of water from the active site[39] and the inability of AutoDock to account for changes in metal coordination.[38] The exclusion of water discounts possible hydrogen bonding interactions, which may occur between the ligand and active site water molecules but the inclusion of water could also block the active site when the ligand displaces water.[38]

3.I.2. Analysis of Specific Ligands

Individual bis-deprotonated ligand poses were analyzed to determine what interactions may lead to ligand binding. Recall, a pose is the conformation of the ligand and flexible amino acid residues in the active site, which is calculated along with that conformation's binding energy by AutoDock. This will be used later to identify differences and similarities in binding between ligands. Hydrogen bonding interactions were examined for individual poses and the orientation of residues observed for each ligand.

3.I.2.a. Myricetin Myricetin binds the strongest to the enzyme with a K_d of 11μM. It was observed that Arginine143 and Lysine 122 interacted significantly with the ligand, with all poses showing some interaction with Arg143 and 10 out of 15 poses showing interactions with Lys122. Enol and S-diketone species were observed to hydrogen bond with the 3 and 4-position oxygens, which may be partially responsible for enzyme inhibition as discussed in section 2.I.1. Some poses also show Arg143 and Lys 136 hydrogen bonding with each side of the B ring (shown in Appendix C), which could explain why myricetin is a stronger binder than quercetin as myricetin has the additional 3'-hydroxyl group on the phenol ring, which permits this interaction. Myricetin was

observed to have a diverse set of poses with no single orientation being repeated multiple times.

3.I.2.b. Quercetin Quercetin also exhibits a diversity in its poses yet consistently has Lys122, Arg143 and Thr 137 oriented toward the ligand with Arg143 contributing significantly to binding with 13 out of 15 poses exhibiting Arg143 interactions. Frequently, in enol and S-diketone species, Arg143 interacts with the 3 and 4- position oxygen while this not observed at all for the R-diketone species. The R-diketone poses show Arg143 interacting with the deprotonated 7-oxygen and lysine with the B ring in such a way that almost sandwiches the ligand. This is occasionally observed in the other species of ligand as well and may contribute to binding.

3.I.2.c. Taxifolin Taxifolin is similar in structure to quercetin as shown in Table 3, with taxifolin differing by a reduction of the enol at the 2-3 bond. This results in taxifolin's inability to tautomerize to the diketone species and results an increase in its observed dissociation constant. Global analysis showed that taxifolin 2S isomers reproduced experimental trends in binding and were analyzed further through trend analysis. This revealed two main clusters of species: the lower energy cluster belonging to 2S3S species and the higher energy cluster belonging to 2S3R species, with the exception of the lowest energy pose overall being 2S3R at -3.97 kcal/mol. This lowest energy pose shows Arg143 hydrogen bonding to the deprotonated 7-oxygen and Lys122 to the deprotonated 4'-oxygen on the phenol, essentially sandwiching the ligand. 2S3S poses showed two main orientations of Arg143: one that maximizes hydrogen bonding of guanidinium hydrogens and the other that appears to be stacking of the guanidinium above the ligand π system suggesting π -cation interactions. 2S3R showed fewer lysine

interactions than 2S3S, suggesting that lysine interactions may lower the binding energy and are involved in binding.

3.I.2.d. Kaempferol Kaempferol is similar in structure to both quercetin and apigenin, where quercetin is a more effective inhibitor and apigenin binds weakly, therefore understanding the interactions between the kaempferol and CuZnSOD could explain this difference. Specific trend analysis shows lysine residues oriented toward the ligand with Lys136 interacting more and Lys122 interacting less with kaempferol than is observed for the other ligands. R-diketone tautomers show fewer interactions with Lys136 than enol and S-diketone forms. Hydrogen bonding with lysine residues may influence binding and if this is the case, enol and S-diketone species would contribute more to binding than R-diketone species.

With kaempferol, significant interactions between the ligand and 3 and 4 position oxygens and either Lys136 or Arg143 are observed in 9 out of 15 poses. An example of this is observed in the comparison between the enol poses with binding energies -2.12 kcal/mol (highest for that species) and -3.29 kcal/mol (lowest for that species). The highest and lowest energy enol poses share very similar ligand orientation and flexible amino acid orientation with the exception of Lys136. In the lower energy pose, Lys136 is oriented toward the 3-hydroxyl group of kaempferol and in the less favorable pose is cantilevered out of the active site away from the ligand. This clearly shows the importance of the Lysine interaction as it results in a 50% decrease in the binding energy, shown below in Figure 18.

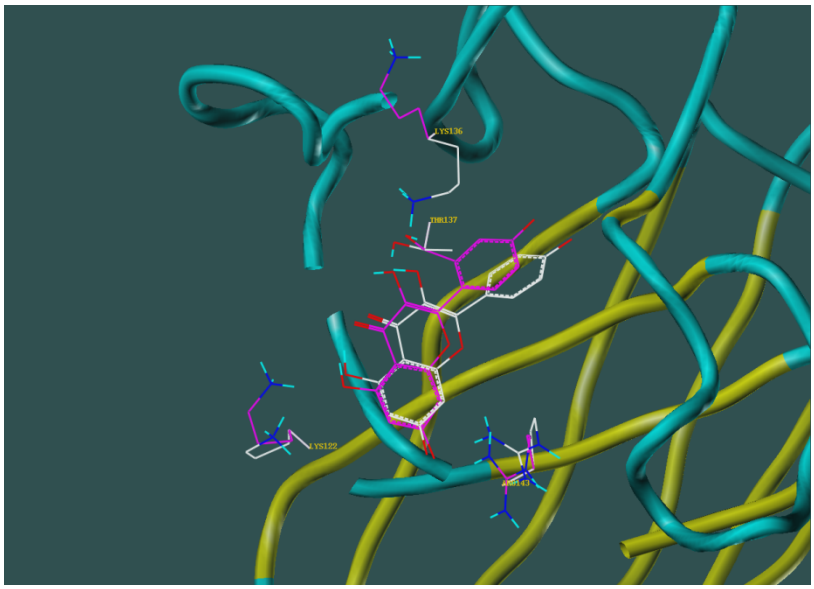

Figure 18. Kaempferol Enol Species Comparison. The -2.12 kcal/mol energy pose (pink) has Lys136 rotated away from kaempferol while the -3.29 kcal/mol energy pose (white) is stabilized through hydrogen bonding of Lys136 to the 3-OH group.

3.I.2.e. Apigenin Apigenin is a poor binder to CuZnSOD with an experimental dissociation constant of 2mM.[30] The global trend analysis predicts apigenin to be a stronger binder than observed experimentally, however individual apigenin poses show fewer interactions than observed for the other flavonols. Lysine 122 and 136 are turned away from the ligand in most poses with 2 out of 5 poses showing no interactions with apigenin. The other three poses show single interactions with Arg143 or Lys136, where arginine hydrogen bonds with either the 1 or 7 position oxygen and lysine to the 4-oxygen. The lack of interactions with lysine residues or with the 3-oxygen may be responsible for its poor binding. The prevalence of these interactions in other stronger binders suggests that they are contributors to the overall binding to CuZnSOD.

3.I.3. Overall Docking Analysis

After individual inhibitors were assessed for hydrogen bonding and residue interactions, trends in binding between those inhibitors were assessed. Several

interactions were observed for flavonols across the board. These included Lysine 122 and Lysine 136 interactions, where Lys122 interactions were observed more for myricetin and quercetin and Lys136 more for taxifolin and kaempferol. This could mean that Lys122 interactions result in stronger binding than Lys136 interactions.

Based on the analysis of poses, we believe that the following interactions are responsible for the observed structure affinity relationship: Arg143 with the 3-oxygen position and Arg143 and lysine interactions with deprotonated 4' and 7-position oxygens. The interactions with Arg143 and lysine have been observed in many poses as previously discussed in Section 3.I.2. Arginine 143 interactions were observed in the majority of poses, where interactions with the 3-oxygen (enol or diketone) correlate well to the experimental binding data as shown in Figure 19.

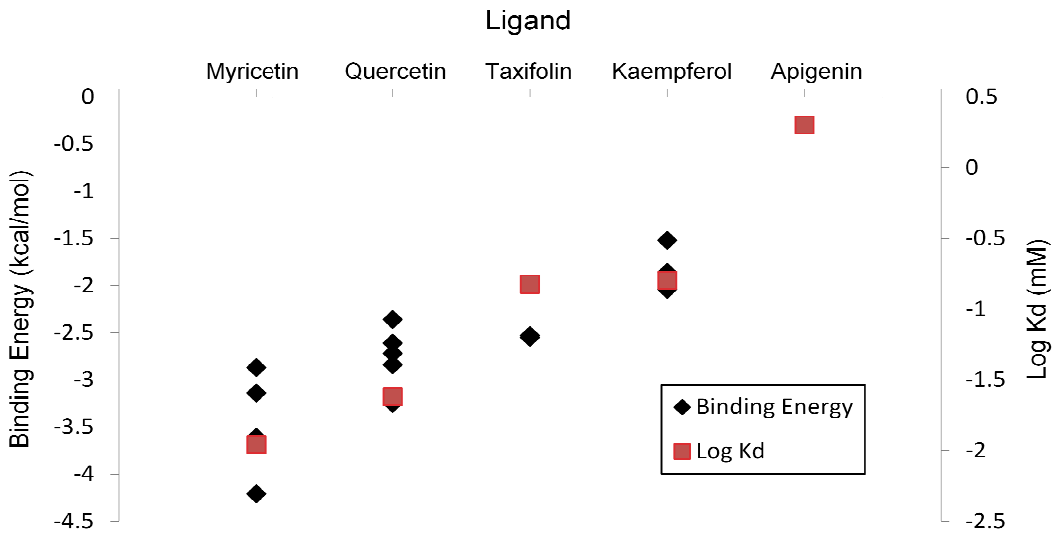

Figure 19. Poses with Arg143 and 3-oxygen Interactions Correlate to Experimental Data.

The correlation of poses with a specific interaction to the experimental data implicates that interaction in the binding of flavonols. Therefore, we believe that interactions between Arg143 and the 3-position oxygen in both enol and S-diketone tautomer species contributes significantly to the binding of flavonols and may explain

why apigenin is not a strong binder of CuZnSOD. We also note the importance of Threonine137 in binding, as poses with Thr137 hydrogen bonding also correlated to experimental binding constants, suggesting that this residue may also assist in overall binding.

3.I.4. Structure Activity Relationship

A qualitative structure activity relationship can be determined based on docking calculations and NMR experimental dissociation constants. Experimental binding data shows myricetin to bind weaker below its pK_a while quercetin[40] does not inhibit at all below its pK_a, this suggests that deprotonated ligands are stronger binders. Docking calculations support this, as trends in the dissociation constant were only observed for bis-deprotonated binding energies. Based on these results, we believe that bis-deprotonated ligands are the state that binds to CuZnSOD. As the pK_a of flavonols is approximately 7, the portion of bis-deprotonated ligand present at pH 8 is very small; however, the binding of the ligand to the enzyme may lower the pK_a because of stabilization of the bis-deprotonation state. The likely tautomer that binds to the receptor may be the enol or the S-diketone tautomer species as R-tautomers are generally higher in binding energy and have less 3-oxygen interactions for myricetin and quercetin and less Lys136 interactions for kaempferol.

The functionality necessary for CuZnSOD inhibition has been demonstrated experimentally. The 3-hydroxyl group absent in the flavonol, apigenin, is necessary for inhibition, as apigenin does not bind where kaempferol binds strongly. The experimental inhibition of CuZnSOD by taxifolin shows that the enol moiety is not necessary for binding but that the reduced 2-3 bond still causes some decrease in effectiveness as compared to quercetin. One goal of docking was to explain this. Interactions with both

the enol and diketone moieties with Arg143 in docking may explain why apigenin does not significantly inhibit CuZnSOD, it does not explain why quercetin is more effectively than taxifolin. One possibility is that the interaction of the diketone with Arg143 is stronger than the enol interaction, so while taxifolin still binds to Arg143, quercetin forms the more energetically favorable interaction explaining its lower K_d value. Another interaction important to binding is the hydrogen bonding of lysine residues and Arg143 with the deprotonated 7 and 4'- positioned oxygens. This sandwiching of the ligand lowers the binding energy and would explain why the bis-deprotonated ligand binds stronger than the neutral and deprotonated species. Threonine 137 is also implicated in binding interactions and binds in the same locations already mentioned.

4. CONCLUSIONS

^{19}F NMR based assaying is an alternative to superoxide generating assays for measuring superoxide dismutase enzyme concentration. We have used this method to screen 500 compounds quickly for CuZnSOD and MnSOD inhibition. None were found to inhibit, but this experiment demonstrates the potential of the assay for high throughput screening. Phytoestrogens were screened for inhibition and it was found that flavonols inhibit CuZnSOD in two steps, the second is only important at alkaline pH.

In this thesis, we have characterized the inhibition of CuZnSOD by a number of flavonols, 9-anthracenecarboxylic acid and acetophenones. The pH dependence of inhibition is consistent with a two-step reaction. The first inhibition step is an equilibrium reaction with a dissociation constant, K_d, of binding that decreases upon deprotonation of the inhibitors. The second inhibition step is a slower reaction that requires deprotonation of the enzyme. We found enzyme deprotonation occurs with a pK_a of 10.1, which correlates to the pK_a of active site residue, Lysine 122.[36] The dependence of initial activity on inhibitor concentration indicates aggregation of flavonols. Absorbance data supported this conclusion. Dimerization is suggested to occur more for deprotonated flavonols than for neutral flavonols.

Also examined in this thesis is the structure activity relationship of flavonol-CuZnSOD binding. NMR assays were used to determine the observed rate constants for various flavonols. We report that taxifolin inhibited CuZnSOD, although less effectively than quercetin. This result indicates that diketone tautomerization is not necessary for binding. To determine whether quercetin covalently modifies CuZnSOD, we analyzed CuZnSOD and quercetin-saturated CuZnSOD samples using mass

spectrometry. No molecular ion or fraction peaks were observed for the quercetin inhibited sample suggesting that the enzyme precipitated from solution after inhibition.

Docking calculations were performed using AutoDock 4.0[23] in order to predict the structure activity relationship of flavonols. We hypothesize that bis-deprotonated ligands bind to the receptor preferentially over neutral and mono-deprotonated forms. Further, enol and S-diketone tautomeric forms are predicted to bind over the R-diketone form. Probable interactions contributing to binding are Arg143 hydrogen bonding with the 3-oxygen and interactions of the deprotonated 4' and 7-position oxygens with Arg143 and lysine residues. An observed discrepancy in the docking calculations was the prediction of apigenin to bind more effectively than shown in NMR experiments. Sources of error include the exclusion of water[38] from the active site, the inability of AutoDock to account for changes in metal coordination, and the exclusion of π -cation interactions.[38]

In conclusion, the inhibition of CuZnSOD by flavonols is a complex system in which both enzyme deprotonation and flavonol deprotonation affect binding. Enzyme deprotonation is not necessary for binding. Deprotonated flavonols are predicted to bind stronger by docking calculations and are observed to do so in NMR experiments. Deprotonated ligands are also likely to aggregate; K_d values are maxima and underestimate the enzyme's affinity for the inhibitor. Our hypothesized structure activity relationship explains the trend in dissociation constants, but more research is needed to determine why quercetin inhibits more effectively than taxifolin.

REFERENCES

[1] Richter, C., Gogvadze, V., Laffranchi, R., Schlupbach, R., Schweizer, M., Sutter, M., Walter, P., Yaffee, M. Oxidants in Mitochondria: From Physiological to Diseases. *Biochim. Biophys. Acta.* **1995,** *1271,* 67.

[2] Fridovich, I. Superoxide Radical and Superoxide Dismutases. *Annu. Rev. Biochem.* **1995,** *64,* 97.

[3] Gutteridge, J. M. C. Superoxide dismutase inhibits the superoxide-driven Fenton Reaction At Two Different Levels: Implications for a Wider Protective Role. *FEBS Letters.* **1985,** *185,* 19.

[4] McCord, J. M., Fridovich, I. The Reduction of Cytochrome c by Milk Xanthine Oxidase. *J. Biol. Chem.* **1968,** *248,* 5753.

[5] Bertini, I., Mangani, S., Viezzoli, M. S. Structure and Properties of Copper-Zinc Superoxide Dismutases. *Adv. Inorg. Chem.* **1998,** *45,*127.

[6] McCord, J. M., Fridovich, I. Superoxide Dismutase: An Enzymatic Function for Erythrocuprein (Hemocuprein). *J. Biol. Chem.* **1969,** *244,* 6049.

[7] Kohanski, M. A., Dwyer, D. J., Hayete, B., Lawrence, C. A., Collins, J. J. A Common Mechanism of Cellular Death Induced by Bactericidal Antibiotics. *Cell* **2007,** *130,* 797.

[8] Huang, P., Oldman, E. A., Keating, M. J., Plunkett, W. Superoxide dismutase as a target for the selective killing of cancer cells. *Nature* **2000,** *407,* 390.

[9] Roberts, B. R., Tainer, J. A., Getzoff, E. D., Malencik, D. A., Anderson, S. R., Bomben, V. C., Meyers, K. R., Karplus, P. A., Beckman, J. S. Structural Characterization of Zinc-Deficient Human Superoxide Dismutase and Implications for ALS. *J. Mol. Bio.* **2007,** *373*, 877.

[10] Soulere, L., Delplace, P., Davioud-Charvet, E., Py, S., Serghepaert, C., Perie, J., Ricard, I., Hoffman, P., Dive, D. Screening of Plasmodium falciparum Iron Superoxide Dismutase Inhibitors and Accuracy of the SOD-Assays. *Bioorg. Med. Chem.* **2003,** *11,* 4941.

[11]Keller, M. J., Bagnell, R., Hale, B., Alexander, N. M., Inactivation of intracellular copper-zinc superoxide dismutases by copper chelating agents without glutathione depletion and methemoglobin formation, *Free Radic. Bio. Med.* **1989***, 6*, 355.

[12]Heikkila, R. E., Cabbat, F. S., Cohen, G. In vivo inhibition of superoxide dismutases in mice by diethyldithiocarbamate. *J. Biol. Chem.* **1976,** *251,* 2182.

[13] Ewing, J. F., Janero, D. R. Microplate Superoxide Dismutase Assay Employing a Nonenzymatic Superoxide Generator. *Anal. Biochem.* **1995,** *232,* 243.

[14] Viglino, P., Rigo, A., Stevanato, R., Ranieri, G. A., Rotilio, G., Calabrese, L. The Binding of Fluoride Ion to Bovine Cuprozinc Superoxide Dismutase as Studied by ^{19}F Magnetic Relaxation. *J. Magn. Reson.* **1979,** *34,* 265.

[15] Unpublished Results.

[16] The Carr-Purcell-Meiboom-Gill experiment is the standard method for measuring transverse NMR relaxation times (T_2). See for example; Braun, S., Kalinowski, H.-O., Berger, S., 150 and More Basic NMR Experiments, Wiley-VCH Weinheim, 1998, page 159.

[17] Rigo, A. Ugo, P., Vigilino, P., Rotilio, G. ^{19}F Nuclear Magnetic Relaxation By Superoxide Dismutase as an Enzymatic Method for the Detection of Superoxide Anion. *FEBS Lett.* **1981,** *132,* 78.

[18] Phytoestrogens studied were: apigenin c, biochanin a, coumestrol, coumestrol dimethyl ether, quercetin, genistein, and daidzein.
[19] Sharma, V., Joseph, C., Ghosh, S., Agarwal, A., Mishra, M., Sen, E. Kaempferol induces apoptosis in glioblastoma cells through oxidative stress. *Mol. Cancer. Ther.* **2007,** *6,* 2544.
[20] Summers, J. S., Baker, J. B., Meyerstein, D., Mizrahi, A., Zilbermann, I., Cohen, H., Wilson, C., Jones, J. Measured rates of fluoride/metal association correlate with rates of superoxide/metal reactions for $Fe^{III}EDTA(H_2O)^-$ and related complexes. J. Amer. Chem. Soc., **2008,** *130,* 1727.
[21] Chalcones prepared are outlined in the appendix and identified as follows: JS MM 8A, 8B, 9A, 9B, and 10A.
[22] DiDonato, M., Craig, L., Huff, M.E., Thayer, M.M., Cardoso, R.M.F., Kassmann, C.J., Lo, T.P., Bruns, C.K., Powers, E.T., Kelly, J.W., Getzoff, E.D., Tainer, J.A. ALS Mutants of Human Superoxide Dismutase Form Fibrous Aggregates Via Framework Destabilization. *J. Mol. Biol.* **2003,** *332,* 601. PubMed DOI: 10.2210/pdb1pu0/pdb.
[23] Huey, R., Morris, G. M., Olson, A. J., Goodsell, D. S. A Semiempirical Free Energy Force Field With Charge-Based Desolvation. *J. Comput. Chem.* **2007,** *28,* 1145.
[24] Musialik, M., Kuzmicz, R., Pawlowski, T. S., Litwinienko, G. Acidity of Hydroxyl Groups: An Overlooked Influence on Antiradical Properties of Flavonoids. *J. Org. Chem.* **2009,** *74,* 2699.
[25] Spartan '04 Wavefunction Inc. Irvine CA. Hehre, W. J. A guide to molecular mechanics and quantum chemical calculations, Wavefunction, Irvine, **2003**.
[26] 1au=1 atomic unit where the energy of a hydrogen atom is -0.5 atomic units. Also, 1 au=2625 KJ/mole. Source: Getting Started with Spartan. 3rd Edition. Wavefunction: Tokyo, Japan, 2002; pp 105.
[27] Sybyl Version 8.1,Tripos, Inc.
[28] Dolinsky, T.J., Nielsen, J. E., McCammon, J. A., Baker, N. A. PDB2PQR: An Automated Pipeline for the Setup, Execution and Analysis of Poisson-Boltzmann Electrostatics Calculations. *Nucleic Acids Res.* **2004,** *32,* W665.
[29] AutoDockTools Version 1.5.2 revision 2. 1999-2008 Molecular Graphics Laboratory. The Scripps Research Institute. Michel F. Sanner. Python: A Programming Language for Software Integration and Development. *J. Mol. Graphics Mod.* **1999**, *17*, 57.
[30] Dissociation constant determined by Jonathan Markley at pH 8. Apigenin dissociation constant an estimated value. Benjamin Hickman and Mandy Nance determined the dissociation constant of 2,4-dihydroxyacetophenone at pH 8 in borate buffer.
[31] Gilbert, H. F. III, O'Leary, M. H. Modification of arginine and lysine in proteins with 2,4-pentanedione. *Biochem.* **1975,** *14(23),* 5194.
[32] Yamasaki, R. B., Vega, A., Feeney, R. E. Modification of available residues in proteins by p-hydroxyphenylglyoxal. *Anal. Biochem.* **1980,** *109,* 32.
[33] DHCH-arginine is N-N-(1,2-dihydroxycyclohex-1,2-ylene)-L-arginine.
[34] Smith, E. L. Reversible blocking at arginine by cyclohexanedione. In *Methods of Enzymology: Enzyme Structure, Part E;* Hirs, C. H. W., Timasheff, S. N., Eds.; Academic Press: New York, 1977; Vol 47, pp 156.
[35] 9-Anthracenecarboxylic acid CAS # 723-62-6. Dictionary of Organic Compounds. ChemNetBase 2010 Taylor and Francis Group. Accessed January 25 2010.
[36] Argese, E., Viglino, P., Rotilio, G., Scarpa, M., Rigo, A. Electrostatic control of the rate-determining step of the copper, zinc superoxide dismutase catalytic reaction. *Biochem.* **1987,** *26,* 3224.

[37] Terenzi, M., Rigo, A., Franconi, C., Mondovi, B., Calabrese, L., Rotilio, G. pH dependence of the nuclear magnetic relaxation rate of solvent water protons in solutions of bovine superoxide dismutase. *Biochim. Biophys. Acta* **1974,** *351,* 230.
[38] Moitessier, N., Englebienne, P., Lee, D., Lawandi, J., Corbeil, C.R. Review: Towards the development of universal, fast and highly accurate docking/scoring methods: a long way to go. *Br. J. Pharmacol.* **2008,** *153,* S7.
[39] Morris, G. M., Goodsell, D. S., Halliday, R. S., Huey, R., Hart, W. E., Belew, R. K., Olson, A. J. Automated Docking using a Lamarckian Genetic Algorithm and an Empirical Binding Free Energy Function. *J. Comput. Chem.* **1998,** *19,* 1639.
[40] Experimental dissociation constants for quercetin above and below its pK_a were determined by Jonathan Markley and are therefore not discussed in other sections of this thesis.

APPENDIX

A. Chalcone Structures Screened for MnSOD Inhibition

8A

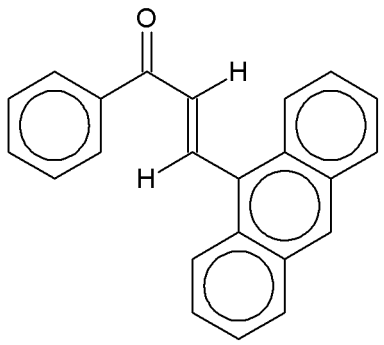

8B

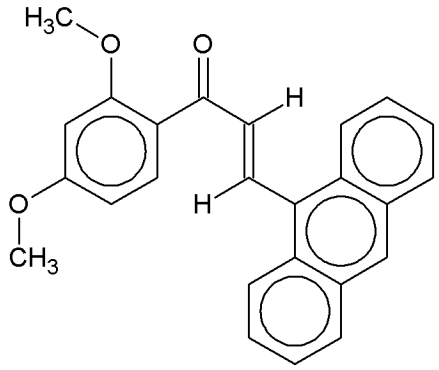

9A

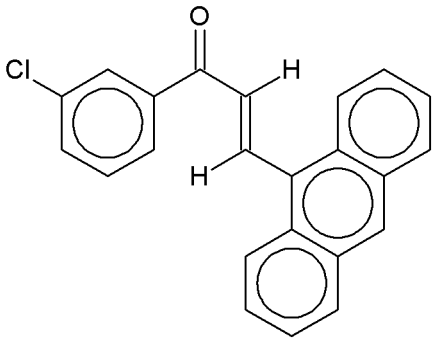

9B

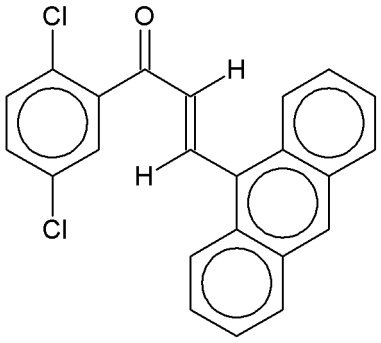

10A

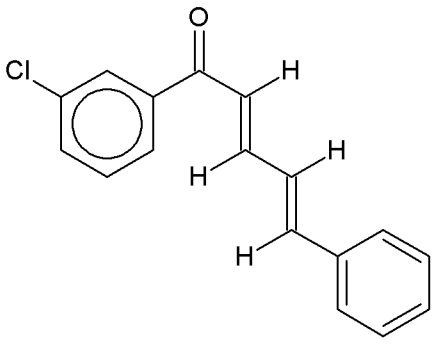

B. Dissociation Constants for CuZnSOD Inhibitors at pH 8[30].

Compound	K_d (mM)
Myricetin	0.011
Quercetin	0.024
Taxifolin	0.150
Kaempferol	0.160
Apigenin	2
DHAP	2.1
THAP	3.5

C. General Flavonol Structure

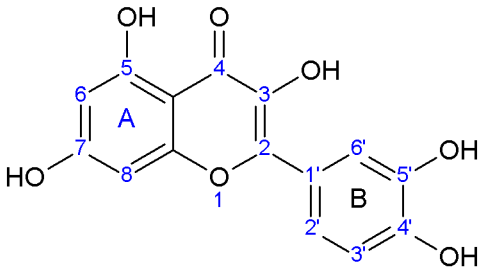

D. Flavonols Screened During the Course of this Project.

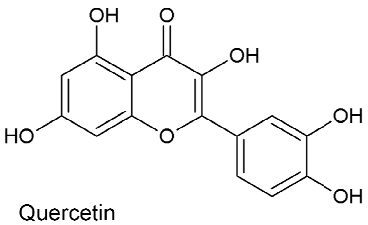

Quercetin

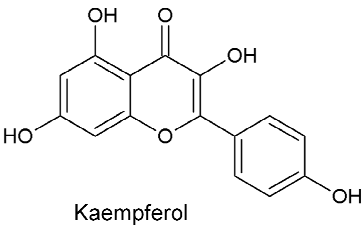

Kaempferol

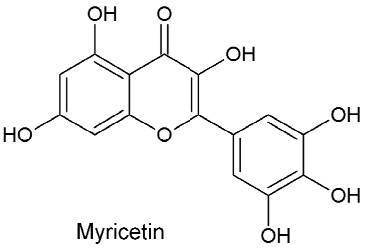

Myricetin

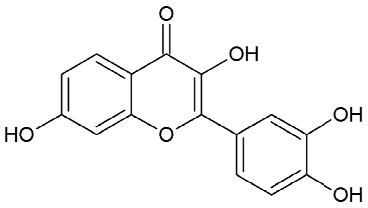

Fisetin

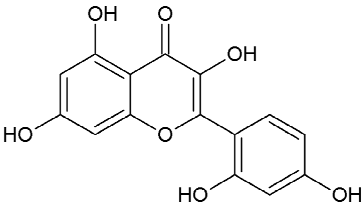

Morin

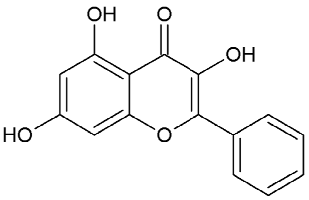

Galangin

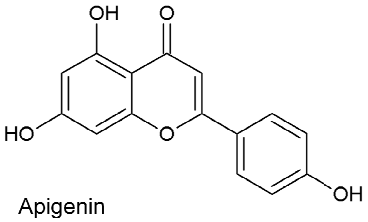

Apigenin

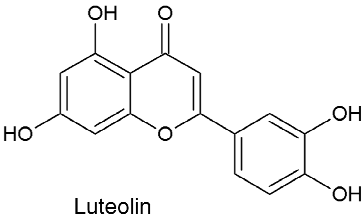

Luteolin

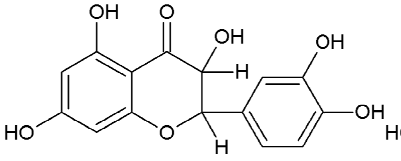

Taxifolin

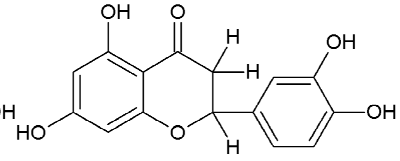

Eriodictyol